Cretaceous Research 140 (2022) 105341

Contents lists available at ScienceDirect

Cretaceous Research

journal homepage: www.elsevier.com/locate/CretRes

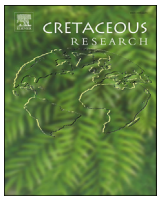

Biostratigraphy, carbon isotope and sequence stratigraphy of South Tethyan Valanginian successions in the Essaouira-Agadir Basin (Morocco)

Stéphane Reboulet [a, *], Etienne Jaillard [b], Majd Shmeit [b, c], Fabienne Giraud [b], Moussa Masrour [d], Jorge E. Spangenberg [e]

[a] Univ. Lyon, Univ. Lyon 1, ENSL, CNRS, LGL-TPE, F-69622, Villeurbanne, France
[b] Univ. Grenoble Alpes, Univ. Savoie Mont Blanc, CNRS, IRD, Univ. Gustave Eiffel, ISTerre, 38000 Grenoble, France
[c] Lebanese University, Doctoral School of Science and Technology, Laboratory of Geosciences, Georesources and Environment (L2GE), EDST/PRASE, Beirut, Lebanon
[d] Université Ibn Zohr, Faculté des Sciences, Département de Géologie, BP 8106, Cité Dakhla, Agadir, Morocco
[e] University of Lausanne, Institute of Earth Surface Dynamics (IDYST), CH-1015 Lausanne, Switzerland

ARTICLE INFO

Article history:
Received 7 March 2022
Received in revised form
5 August 2022
Accepted in revised form 19 August 2022
Available online 30 August 2022

Keywords:
Ammonite
Calcareous nannofossil
Depositional sequence
Weissert Event
Morocco
Inter-basin correlation

ABSTRACT

A detailed stratigraphic analysis was carried out on Valanginian deposits of six Moroccan sections of the Essaouira-Agadir Basin (EAB, South Tethyan margin) in order to characterize the Weissert Event and propose correlations with the North Tethyan margin (south–east France Basin). The studied successions consist of alternating marlstone and limestone beds with sandy intercalations, and are well exposed and relatively rich in ammonites. Ammonite biostratigraphy and sequence stratigraphy were established for all successions, whereas calcareous nannofossil and carbon stable isotope analyses were performed for two and five sections, respectively. For each succession, an accurate ammonite zonal scheme allows to recognize the standard zonation established for the Mediterranean Province. A calcareous nannofossil zonation is provided for Zalidou and Aït Hamouch, considered as reference sections. The detailed biozonations allowed to ascribe an accurate age for most of the sedimentary discontinuities and depositional sequences identified in the EAB. East–west and north–south transects are established for the Valanginian depositional system. Despite some stratigraphic gaps, the Valanginian carbon isotope excursion (CIE) was recognized in most of the studied sections. The Moroccan successions are correlated with those of reference sections of south–east France i.e., the Vocontian Basin (Vergol-La Charce) and Provence Platform (Carajuan), using bio-sequence-chemo-stratigraphy. These inter-basin correlations allowed to evidence major "mid-Valanginian" and upper Valanginian eustatic regressions; the possible role of tectonics and glacio-eustacy is also discussed.

1. Introduction

Several significant palaeoceanographic, palaeoclimatic and palaeoenvironmental changes are recorded in Valanginian times (Gale et al., 2020). The South Atlantic Ocean began to open and the early stages of rifting were accompanied by extrusion of the Parana-Etendeka large igneous province (Coffin and Eldholm, 1994; Gomes and Vasconcelos, 2021). A cooling of the climate is recorded at least locally (Price, 1999; Pucéat et al., 2003). A biosphere crisis is suspected through a global carbon-cycle perturbation recorded by positive carbon isotope excursion in marine carbonates and terrestrial organic matter, named the Valanginian Weissert oceanic anoxic event or the Weissert Event (Erba et al., 2004; Gröcke et al., 2005; Kujau et al., 2012). For these reasons, Valanginian successions have been extensively studied in the North Tethyan margin, where numerous detailed lithological, biostratigraphic, sedimentological and isotopic data are available (Lini et al., 1992; Föllmi et al., 1994; Hennig et al., 1999; Sprovieri et al., 2006; McArthur et al., 2007; Gréselle et al., 2011; Charbonnier et al., 2017; Aguado et al., 2018). As a result, reference sections are mainly located in south–east France, such as Vergol (Montbrun-les-Bains, Drôme),

* Corresponding author.
E-mail address: stephane.reboulet@univ-lyon1.fr (S. Reboulet).

https://doi.org/10.1016/j.cretres.2022.105341
0195-6671/

candidate section for the Valanginian Global Boundary Stratotype Section and Point (GSSP, Blanc et al., 1994; Kenjo et al., 2021) and La Charce (Drôme), GSSP for the Hauterivian (Mutterlose et al., 2020). Elsewhere, however, integrated studies are quite rare (e.g., Aguirre-Urreta et al., 2019), and works on the Valanginian period focused on ammonite biostratigraphy (e.g., Rawson, 2007), calcareous nannofossils zonation (e.g., Bralower, 1987; Bralower et al., 1989), synsedimentary tectonics (e.g., Masse and Lesbros, 1987; Gradinaru et al., 2016), sedimentary geochemistry and palaeoclimatology (e.g., Pucéat et al., 2003; Charbonnier et al., 2020).

In the South Tethyan margin of Africa, Lower Cretaceous deposits are commonly represented by clastic subaerial sediments ("Continental Intercalaire", Lefranc and Guiraud, 1990; Fanti et al., 2012; Newell et al., 2015), and marine sediments are restricted to the distal parts of the North-African margin. However, the latter are often deformed by the Alpine orogeny (Frizon de Lamotte et al., 2000) that makes difficult their study. Therefore, the Valanginian series are poorly known, and the Weissert Event is not documented by carbon isotope data, in spite of some integrated stratigraphy studies in northern Tunisia (Soua, 2016; Melliti et al., 2019; Ben Ammar and Layeb, 2021). The Moroccan Essaouira-Agadir Basin is located at the western edge of the High Atlas Mountain Range and on the Atlantic coast of Morocco. The basin belonged, therefore, to the southern margin of the Mesozoic Tethys Ocean. It offers a rare opportunity to study the Valanginian stage, since it presents excellent outcrops ranging from outer shelf to nearshore environments (Ferry et al., 2007) and the Valanginian successions are rich in ammonites (Wippich, 2003; Ettachfini, 2004). Recently, the mid–Valanginian carbon isotope excursion has been identified for the first time in the deposits of the Essaouira-Agadir Basin (Shmeit et al., 2022). Six sections located in this basin provide ideal successions for an integrated approach owing to the well-exposed outcrops and relatively abundant ammonite records. The sections were also chosen to establish two transects: one in a south–north direction with Aït Hamouch, Zaouia Sidi Abderahmane and Zalidou; and one in a west–east direction with Obbay, Igouzoulen and Ida w Iddar. Except for the two latter sites, the successions were studied mainly for the ammonite content by Wippich (2001, 2003) and/or Ettachfini (2004).

The main goals of the study were: (1) to establish a well-constrained integrated stratigraphic framework of the upper Berriasian–lowermost Hauterivian interval of the Essaouira-Agadir Basin, based on a high-resolution biostratigraphy involving ammonite and calcareous nannofossil biozonations, and carbon isotope stratigraphy, thus allowing a characterization of the Weissert Event in the South Tethyan margin; (2) to define time lines, based on the analysis of the evolution of sedimentary depositional environments, discontinuity surfaces and sequence analysis; and (3) to correlate the studied sections of the Essaouira-Agadir Basin with those of south–east France Basin in order to discriminate local from global factors, that influence sedimentary palaeoenvironments.

To shorten the manuscript, some abbreviations are used. Essaouira-Agadir Basin, EAB. South–east, SE. Formation, Fm. Sequence boundary, SB. "Discontinuité du Valanginien moyen", DVM. "Discontinuité du Valanginien supérieur", DVS. "Discontinuité du Valanginien terminal", DVT. "Discontinuité au toit des Calcaires Blancs", DCB. Hummocky cross stratification, HCS. First occurrence, FO. Last occurrence, LO. First appearance datum, FAD. Last appearance datum, LAD. For the ammonite zonation: Standard zone, StZ; Standard subzone, StSz; Local subzone, LSz. Carbon isotope excursion, CIE. Deep Sea Drilling Project, DSDP. For the stratigraphic position of fossils, an alphanumeric notation is used with the abbreviation of the name of the section followed by the bed number: Aït Hamouch, AH or AtH; Zalidou, ZA; Zaouia Sidi Abderahmane, ZS; Igouzoulen, IGb or IGz; Ida w Iddar, IW; Obbay, OB.

2. Geological setting

The EAB belongs to the Western Atlas Chain. It is part of the Atlantic passive margin, the evolution of which can be divided into a rifting phase (Late Permian–Late Triassic), a drifting phase (Early Jurassic–Turonian) and an Atlasian deformation period. The first compressional deformation was of Santonian–Campanian age, followed by the Eocene–Pleistocene Alpine deformation which gently folded the EAB (Guiraud and Bosworth, 1997; Algouti et al., 1999; Frizon de Lamotte et al., 2000, 2009; Zühlke et al., 2004; Hafid et al., 2008). During the Early Cretaceous, the EAB was dominated by an extensional regime (Le Roy et al., 1998) and a low thermal subsidence rate (Ellouz et al., 2003; Bouatmani et al., 2007). After drowning of the Upper Jurassic–Berriasian carbonate shelf, deposition in the EAB is first dominated by marl accumulation with scarce limestone beds (Valanginian–Hauterivian), then by a marlstone-limestone succession (Barremian–Aptian) with a coarse sandy intercalation (upper Barremian) and finally, by a thick shaly series (Albian) capped by upper Albian limestones (Ambroggi, 1963; Wiedmann et al., 1982; Canérot et al., 1986; Rey et al., 1988; Witam, 1998; Bourgeoini et al., 2002; Ferry et al., 2007; Luber et al., 2017; Jaillard et al., 2019a, 2019b; Gale, 2020).

In the EAB, west-sloping Mesozoic strata rest on the Hercynian rocks of the High Atlas (Fig. 1). The EAB comprises two main, east–west trending folds, which divide it in three parts. The southern part constitutes the southern flank of the Imouzzer anticline, the core of which offers large outcrops of Jurassic rocks. The central part is comprised between the Imouzzer and the Amsittene anticlines, and includes a mild anticline located south of Tamanar (Fig. 1). The northern part is located north of the Amsittene anticline and has not been studied here.

The first comprehensive works to understand the stratigraphy of the EAB were by Roch (1930) and Ambroggi (1963) who provided major contributions, and Duffaud et al. (1966). An overview of the Cretaceous sedimentary succession of the EAB has been given by Wiedmann et al. (1982). According to Duffaud et al. (1966), Rey et al. (1986, 1988) and Taj-Eddine et al. (1992), the uppermost Tithonian–lowermost Hauterivian interval comprises four formations (Fig. 2). The Cap Tafelney Fm is made of bryozoan-rich limestones overlain by calpionellid-rich limestone beds, which allowed to ascribe the unit to the uppermost Tithonian–Berriasian. The fossiliferous Aghroud Oudar Fm (lower Valanginian), comprises alternating marlstone and argillaceous limestone beds. The Sidi Lhoussaine Fm, ascribed to the upper Valanginian and lower Hauterivian, consists of green marlstone, with few limestone beds at the base and sand beds at the top. The Tamanar Fm (lower Hauterivian), is defined as a reefal limestone unit. The limits of these units, however, are not well defined.

Detailed palaeontological studies based on ammonites of the uppermost Berriasian–lowermost Hauterivian interval have been performed by Ettachfini (1991, 2004) and Wippich (2001, 2003). Their rigourous works on the systematics of Valanginian fauna allowed to show taxonomic misinterpretations of some Valanginian neocomitids and olcostephanids, and to propose new biochronostratigraphic results. For example, Wippich (2003) recognized most of the ammonite (sub-)zones of the standard zonation of the Mediterranean Province proposed by Hoedemaeker et al. (2003). Wippich (2003) identified, for the first time, ammonite markers to characterize the Valanginian–Hauterivian boundary that is placed within a thick marly series corresponding to the Sidi Lhoussaine Fm of Rey et al. (1986, 1988).

From a sedimentological point of view, Rey et al. (1986, 1988) identified two major sedimentary discontinuities, at the top of the Berriasian Cap Tafelney Fm, and at the base of the lower Hauterivian Tamanar Fm, respectively. Minor discontinuities are also

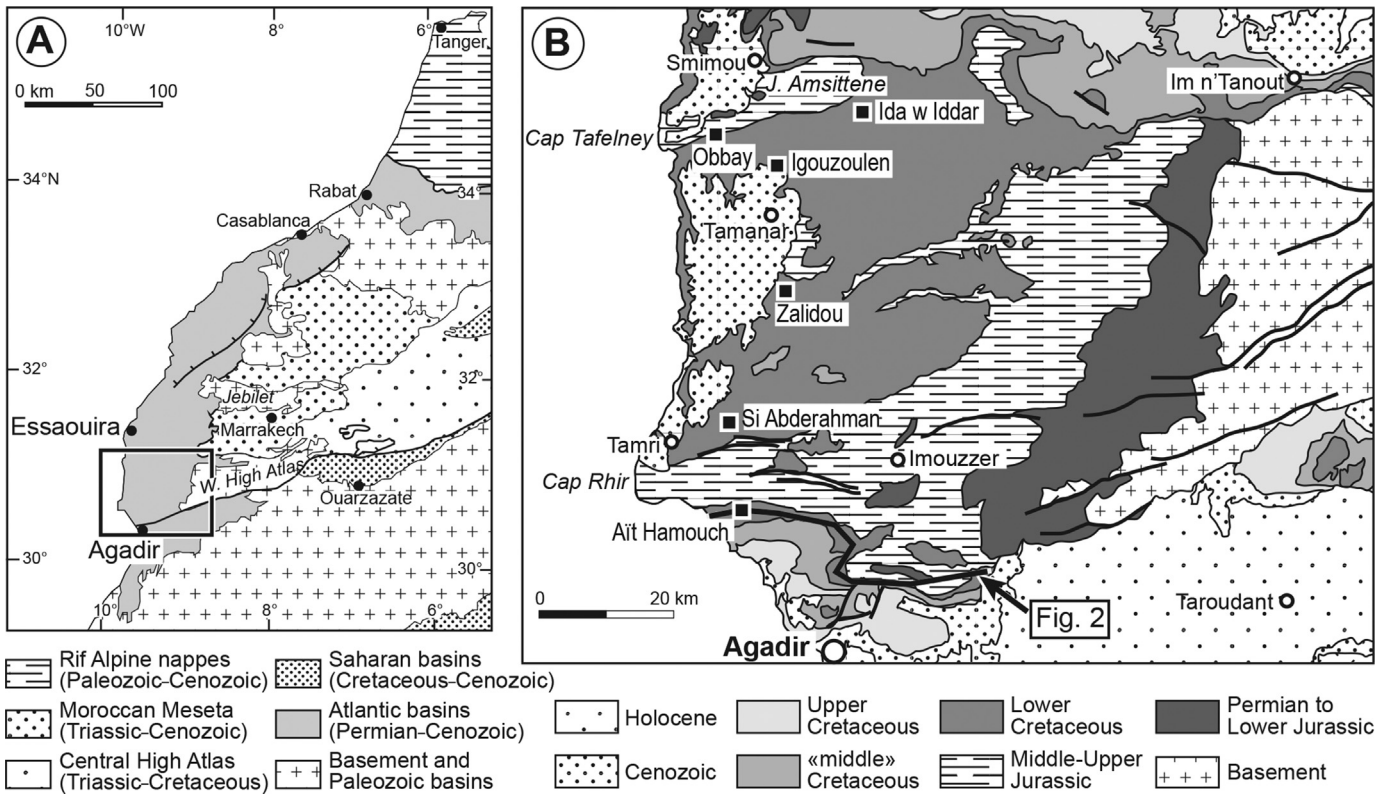

Fig. 1. Location of the study area. A. Location of the Essaouira-Agadir Basin (EAB). B. Geological sketch of the EAB, and location of the studied sections (black squares). The east–west transect of sections illustrated in Fig. 2 is represented by a black line.

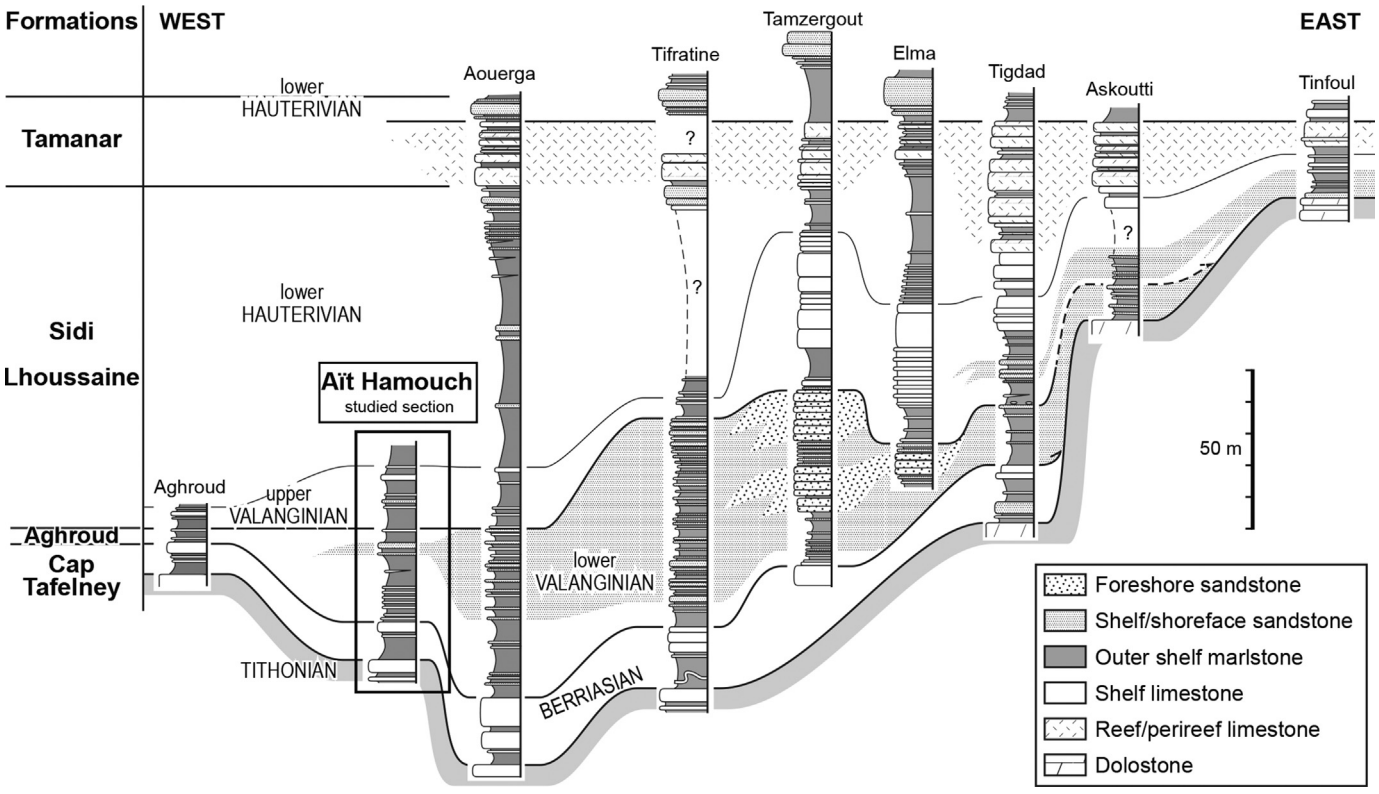

Fig. 2. The Berriasian–lower Hauterivian sedimentary evolution in the southern part of the Essaouira-Agadir Basin. Simplified from Ferry et al. (2007). Note the eastward retrogradation of facies during the Berriasian–upper Valanginian interval, and the westward progradation in the lower Hauterivian. Among the successions illustrated here, only Aït Hamouch was selected for the present work.

mentioned in the upper part, and at the top, of the Aghroud Oudar Fm (lower Valanginian), and within the Sidi Lhoussaine Fm (upper Valanginian–lower Hauterivian). These authors also determined a transgressive trend at the base of the Valanginian, and a transgressive trend through Valanginian times, locally interrupted by an emergence period near the lower–upper Valanginian boundary. Ferry et al. (2007) provided detailed, well-dated sections of the Berriasian–Hauterivian series (Fig. 2). They interpreted the Valanginian series as deposits of a shallow mixed, carbonate-clastic shelf. According to these authors, the Berriasian and lower Valanginian deposits are an overall east-ward retrograding system. The base of the upper Valanginian shows a significant transgressive trend, and the lowermost Hauterivian is marked by a sudden subsidence pulse which causes a new transgression, followed by a major progradation in the upper part of the lower Hauterivian (Fig. 2; Ferry et al., 2007).

3. Materials and methods

Among the six studied sections, one is located in the southern part of the basin, while the other sections belong to its central part; their GPS coordinates are given in Appendix A (Tab. A1, Supplementary material). Altogether, they define a north–south and an east–west profile (Fig. 1). These sections correspond to the external part of the EAB. For an east–west profile of the southern part of the EAB, see Ferry et al. (2007). The Zalidou section is located north–east of the village Ida w Tghouma and was already described by Ettachfini (2004). The Aït Hamouch and Zaouia Sidi Abderahmane sections are located on the southern and northern side of the Imouzzer anticline, respectively. The former was described by Wippich (2001, 2003), Ettachfini (2004) and Ferry et al. (2007), and the latter corresponds to the Zaouia Sidi Abder-Rahmane and Taourirt Oubazine sections of Wippich (2001, 2003) and to the Zawiat Si Abd A-Rahmane of Ettachfini (2004). The Igouzoulen section has been studied along the Igouzoulen river, a few km west of the Tamanar-Smimou road. The Ida w Iddar and Obbay sections belong to the southern flank of the Amsittene anticline. The latter was already studied by Ettachfini (2004).

The fossils and rock samples were collected in Morocco and exported in France within the framework of the project "MA/13/291-PHC-Volubilis" and according to the national legislation of Moroccan authorities; documents and sampling-export certifications are given in Appendix B (Supplementary material).

3.1. Sedimentology

The sections were studied and measured bed by bed. Most sedimentological observations (lithology, texture, sedimentary features, macrofossil content, bioturbation, minerals) were made on the field. Samples were collected in limestone beds, and thin sections were prepared for microfacies analysis. Because the Valanginian–lowermost Hauterivian succession is mainly made of marlstone, facies were chiefly defined through field observations, locally completed by few microfacies analysis of limestone beds.

3.2. Ammonites

1344 specimens of ammonites were recolted in the six studied sections; no aptychus has been observed. The sampling was mainly done from Valanginian limestone beds. The uppermost part of the Berriasian and the basal part of the Hauterivian were also sampled in some sections. Only specimens well-preserved enough to allow an identification were transferred to the laboratory (Lyon, France), where extraction was completed using a vibratory device, and determination was effectuated using a palaeontological worksheet. Specimens doubtfully identified are indicated by a question mark. Dissolution of shells is usual and ammonites are generally preserved as internal calcareous moulds. Lower Valanginian ammonites are relatively well preserved and may reach a large size. Upper Valanginian specimens are more often fragmented and crushed. A few dozens of pyritized specimens were found in marlstone of the upper Valanginian. The specimens are recorded as "Collection Reboulet" with the label "UJF-ID" that means "Université Joseph Fourrier – Institut Dolomieu" belonging to the OSUG Collections; OSUG-COLLECTIONS is a database of rocks, minerals and fossils (https://web.collections.osug.fr, OSUG, UGA. https://doi.org/10.5072/OSUG-COLLECTIONS.all).

3.3. Calcareous nannofossils

A total of 90 and 55 samples, selected from calcareous clay to limestone, and collected in the Zalidou and Aït Hamouch sections, respectively, were investigated for calcareous nannofossil biostratigraphy (Shmeit et al., 2022; this work). These two sections are more extended and are characterized by more marly intervals with respect to the other sections; and were, therefore, more suitable for nannofossil sampling. Studied samples from the composite Aït Hamouch section corresponded to the "AH" section, except for the interval between 32 and 42 m, where the studied samples were collected from the "AtH" section. Methods of smear slide preparation, counting and evaluation of the nannofossil preservation, as well as taxonomic framework and zonations used here were described in Shmeit et al. (2022). The smear slides are numbered as "UJF-ID" (Université Joseph Fourrier – Institut Dolomieu) and curated in the OSUG Collections (for the database, the URL is indicated in Secction 3.2).

3.4. Carbon stable isotopes

The analysis was performed on 291 whole rock samples from the studied sections, except Obbay, at the stable isotope laboratories of the Institute of Earth Surface Dynamics of the University of Lausanne. Analyses where done using a Thermo Fisher Scientific Gas Bench II carbonate preparation device connected to a Delta Plus XL isotope ratio mass spectrometer. The CO_2 extraction was done at 70 °C. The carbon isotope ratios were reported in the delta (δ) notation as the per mil (‰) relative to the Vienna Pee Dee belemnite standard (VPDB), where $\delta = (\text{Rsample} - \text{Rstandard})/\text{Rstandard}$ and $R = {}^{13}C/{}^{12}C$. The measured $\delta^{13}C_{carb}$ values were normalized to the VPDB scale by calibration of the reference gases and working standards with international reference materials NBS 18 (carbonatite, $\delta^{13}C = -5.01‰$) and NBS 19 (limestone, $\delta^{13}C = +1.95‰$). Analytical uncertainty (1 sigma), monitored by replicate analyses of the international calcite standard NBS 19 and the laboratory standard Carrara Marble ($\delta^{13}C = +2.05‰$) was not greater than ±0.05‰ for $\delta^{13}C$.

4. Results and interpretations

4.1. Ammonite stratigraphy: zonation and chronostratigraphic subdivisions

The ammonite fauna of the six studied Moroccan sections (Figs. 3–8) consists of 33 genera grouped into 7 families, using the supra-classification proposed by Klein (2005) and Klein et al. (2007, 2009), partly modified. The classification used here and the authorship of generic and specific names are shown in the taxonomic list provided in Appendix C (Supplementary material). The systematic revision of species was mainly based on the monographies of Le Hégarat (1973), Company (1987), Bulot (1995),

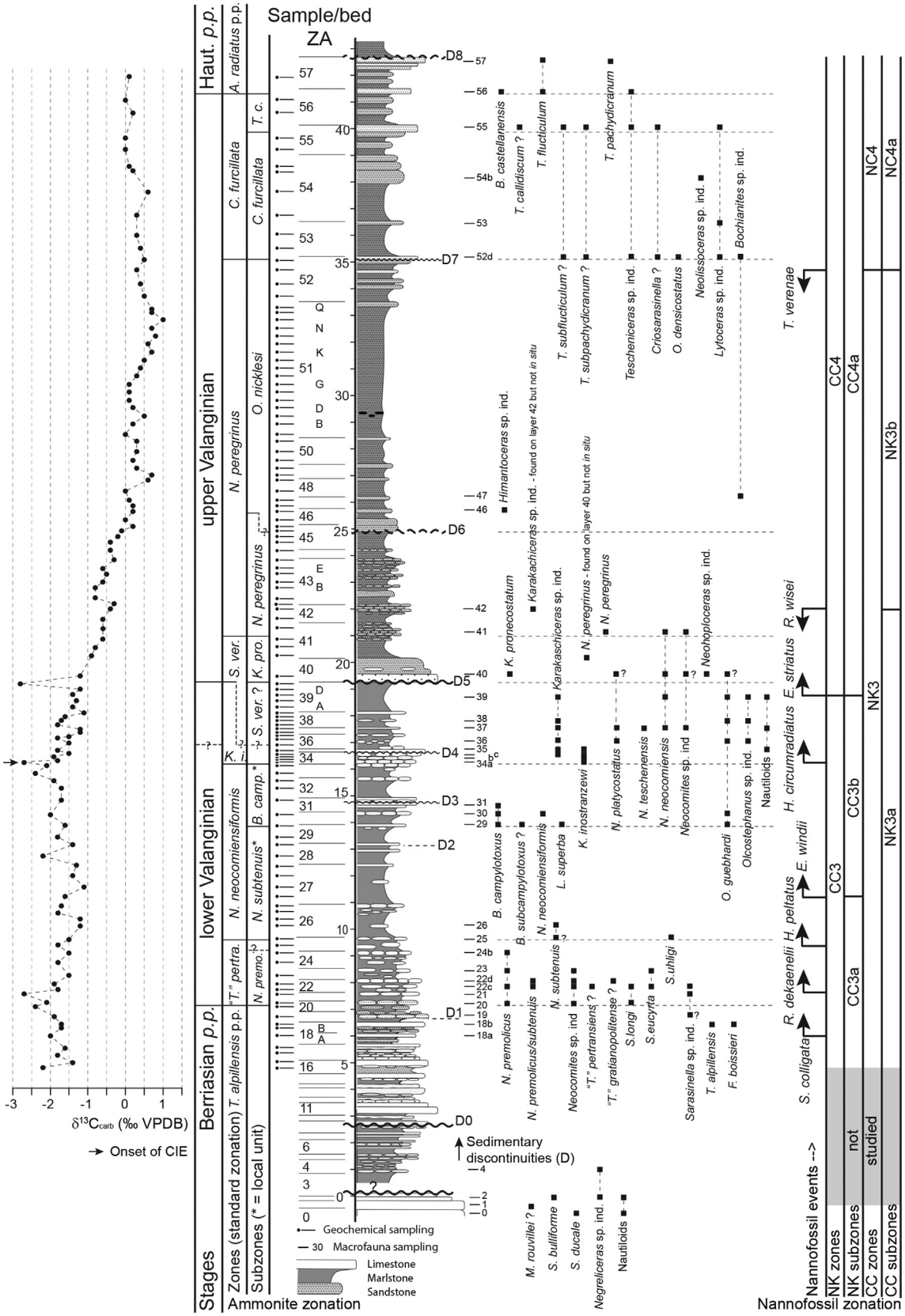

Fig. 3. The Zalidou section. Stratigraphic distribution of macrofauna (mainly ammonites; a question mark is added when identification is doubtful) and ammonite zonation (standard and local units); layers of sampling are indicated at the right of the succession. Nannofossil zonation (NK, NC and CC) and bioevents (FO and LO) from Shmeit et al. (2022) and completed in this work. The NK and NC zones are from Bralower (1987), Bralower et al. (1989, 1995), modified from Roth (1978). The CC zones and subzones are from Sissingh (1977), modified by Perch-Nielsen (1979, 1985) and Applegate and Bergen (1988). Sedimentary discontinuities (D). Carbon isotopic curve; layers of sampling are indicated at the left of the succession. The lower–upper Valanginian boundary is preferentially placed at the base of layers ZA40 (boundary indicated by a solid line); an alternative proposal (ZA36, boundary indicated by a dashed line) is discussed in the text (see Section 4.1).

Reboulet (1996), Joly (2000), Wippich (2001), Ettachfini (2004), Busnardo (*in* Gauthier et al., 2006) and Kenjo (2014). Further information on stratigraphy and taxonomy is available in the papers by Thieuloy (1977), Busnardo and Thieuloy (1979), Thieuloy et al. (1990), Reboulet et al. (1992), Thieuloy and Bulot (1992), Bulot et al. (1993), Bulot and Thieuloy (1995), Aguirre-Urreta and Alvarez (1999), Reboulet and Atrops (1999), Busnardo et al. (2003), Wippich (2003), Reboulet (2008), Company and Tavera (2015), Mourgues et al. (2015), Aguado et al. (2018) and Vašíček (2020). Palaeontological comments and illustrations are given for some taxa in Appendix D (text and Figs. D1–D7, Supplementary material).

The analysis of the ammonite stratigraphic distribution allowed to establish a zonal scheme for the studied sections. The standard ammonite zonation built by the International Union of Geological Sciences Kilian Group (Hoedemaeker et al., 2003; Reboulet et al., 2006, 2009, 2011, 2014, 2018) for the Mediterranean Province of the Mediterranean–Caucasian Subrealm (Tethyan Realm) is applied here. Only two regional units are added, namely the *N. subtenuis* and *B. campylotoxus* local subzones, in order to make easier the comparisons with previous works of Wippich (2001, 2003) and Ettachfini (2004). The ammonite zones are interval zones and are defined by the interval between the FAD of two successive ammonite-indices (Hedberg, 1976). In order to correlate more precisely biostratigraphic subdivisions with ammonite evolution, the boundaries of the Valanginian interval zones correspond to major changes in the ammonite fauna (Reboulet and Atrops, 1999; Kenjo, 2014; Company and Tavera, 2015; Kenjo et al., 2021); this allows a better faunal characterization of the zones. The chronostratigraphic subdivisions (Berriasian–Valanginan, lower–upper Valanginian and Valanginian–Hauterivian boundaries) are characterized in terms of ammonite markers.

The *Tirnovella alpillensis* Standard Zone – uppermost Berriasian. According to the Kilian Group (Reboulet et al., 2018), the *T. alpillensis* StZ is the last zone of the Berriasian (for detailed information see Kenjo et al., 2021). The index-species was found in the Zalidou, Zaouia Sidi Abderahmane and Obbay sections (Figs. 3, 5, 8). However, as the sampling was low in the lower part of the successions, the FO of *T. alpillensis* cannot be used here to place the base of the zone. Also, the *T. alpillensis* StZ is more or less well-recognized in the studied sections by the occurrence of some quite characteristic taxa of the upper Berriasian like *Fauriella boissieri*, *Berriasella calisto*, *Malbosiceras rouvillei*, *Pomeliceras breveti*, *Spiticeras bulliforme*, *Spiticeras ducale*, *Kilianiceras gratianopolitense*, *Negreliceras* sp., *Groebericeras* sp., *Ptychophylloceras (Semisulcatoceras) semisulcatum, Holcophylloceras silesiacum* and *Lytoceras honnoratianum*.

The "*Thurmanniceras*" *pertransiens* Standard Zone and the *Neocomites premolicus* Standard Subzone – Base of the Valanginian stage. Few specimens of "*T.*" *pertransiens* were found in the Zalidou, Aït Hamouch, Igouzoulen and Obbay sections (Figs. 3–4, 6, 8). In the latter site, the FO of this index-species is used to identify the base of the "*T.*" *pertransiens* StZ and thus the lower boundary of the Valanginian (OB13). Kenjo et al. (2021) discussed the choice of the primary marker to define the base of this stage, and gave the priority to the FAD of "*T.*" *pertransiens* rather than the FAD of *Calpionellites darderi*. As the index-species of "*T.*" *pertransiens* is rare or even absent in most of the Moroccan sections, the base of the zone can be placed with the FO of *N. premolicus* (Ettachfini, 2004; this work, ZA20, AH60, ZS34, IGz18; IW5; Figs. 3–7). Taking in account the systematic and biostratigraphic characteristics of *N. premolicus* shown by Ettachfini (2004), Kenjo (2014) and Company and Tavera (2015), the Kilian Group agreed to introduce the *N. premolicus* Subzone in the standard zonation (Reboulet et al., 2018). This subzone starts at the base of the "*T.*" *pertransiens* StZ and ends at the LO of *N. premolicus*. Because the upper part of the zone is not characterised by a subzone for the moment, the *N. premolicus* StSz is provisionaly considered as a total range subzone. For Wippich (2003), the simultaneous FO of *N. premolicus* and the genus *Sarasinella* is a workable alternative to put the base of the "*T.*" *pertransiens* StZ. Except for *Sarasinella trezanensis* that would appear in the uppermost part of the Berriasian, Ettachfini (2004; tab. 5, p. 82) also noted the co-occurrence of "*T.*" *pertransiens*, *N. premolicus*, *Sarasinella eucyrta* and *Sarasinella longi* at the base of the Valanginian. The simultaneous FO of *N. premolicus* with *S. longi* or *S. eucyrta* are recorded at the base of the "*T.*" *pertransiens* StZ in the Zalidou and Aït Hamouch sections, respectively (Figs. 3–4). These two species of *Sarasinella* and *S. trezanensis* are also recorded in the rest (mainly in the lower part) of the "*T.*" *pertransiens* StZ in most of the studied sections (Figs 3–5, 7–8). In most of the Moroccan studied sections (Figs. 3–6, 8), *"Thurmanniceras" gratianopolitense* takes place in the "*T.*" *pertransiens* StZ; in Aït Hamouch, Igouzoulen and Obbay sites, this species first occurs at the base of the zone. Considering that the specimens of *"Thurmanniceras" thurmanni* studied by Wippich (2001, 2003) may be (partly?) interpreted as "*T.*" *gratianopolitense* (see Kenjo et al., 2021), it seems that this species could appear in the *T. alpillensis* StZ as shown in figures of synthetic ranges of taxa provided by Wippich (2001, tab. 15; 2003, fig. 10). According to his sections showing ammonite ranges, "*T.*" *thurmanni* occurs in the "*T.*" *pertransiens* StZ, except in Addar, where the appareance of "*T.*" *thurmanni* occurs in bed 105 dated from the uppermost part of the Berriasian by this author. The specimen illustrated in Wippich (2001, "*T.*" *thurmanni*, pl. 20, fig. 1) and sampled in layer 105 is here interpreted as "*T.*" *gratianopolitense*. The layer 105 of Wippich (2001) could be dated from the "*T.*" *pertransiens* StZ as the last typical Berriasian taxa occur in layer 104 and the first typical Valanginian taxa appear just above in layer 106. Moreover, it seems that Wippich (2001, 2003) identified the base of the "*T.*" *pertransiens* StZ in the Aït Hamouch section with the FO of his "*T.*" *thurmanni*. Ettachfini (2004; tab. 5) also indicated the occurrence of "*T.*" *gratianopiltense* in the uppermost part of the Berriasian. In his sections showing the ammonite distributions (Addar, Sidi Yahia Ou Saïd, Zalidou, and Akoui Griz), specimens of this species were found in the top part of the *T. alpillensis* Subzone; however, at least for some of these sections, this interval could be alternatively dated as lowermost Valanginian. The difference in the ranges of "*T.*" *gratianopolitense* (Wippich (2001, 2003) and Ettachfini (2004) *versus* Company and Tavera (2015) and this work), may be also explained by a different conception of this species. Four specimens of *Thurmanniceras*? were found in the *T. alpillensis* StZ of the Ida w Iddar section (Fig. 7, IW2b); they may correspond to true "*T.*" *thurmanni*, as this species is recorded in the uppermost part of the Berriasian by Ettachfini (2004). These comments on the stratigraphic distribution of *Thurmanniceras* around the Berriasian–Valanginian boundary interval show that a revision of this genus is needed. Regarding *Kilianella*, this genus is only observed in the upper part of "*T.*" *pertransiens* StZ in the Aït Hamouch (Fig. 4) and Ida w Iddar sections (Fig. 7; one specimen of *Kilianella lucencis*?). This is in accordance with other data on the Moroccan western High Atlas given by Ettachfini (2004; occurrence of *Kilianella* sp. 1 in the upper part of his *N. premolicus* Zone); Wippich (2001, 2003) did not record *Kilianella* in the "*T.*" *pertransiens* StZ. In summary, the (co-) occurrences of "*T.*" *pertransiens*, "*T.*" *gratianopolitense*, *N. premolicus*, *S. longi* and/or *S. eucyrta* allow to place the base of the Valanginian and provide a good characterisation of the "*T.*" *pertransiens* StZ of all the studied sections (Figs. 3–8).

The *Neocomites neocomiensiformis* Standard Zone; *Neocomites subtenuis* and *Busnardoites campylotoxus* local subzones. The *N. neocomiensiformis* StZ is applied for the first time in

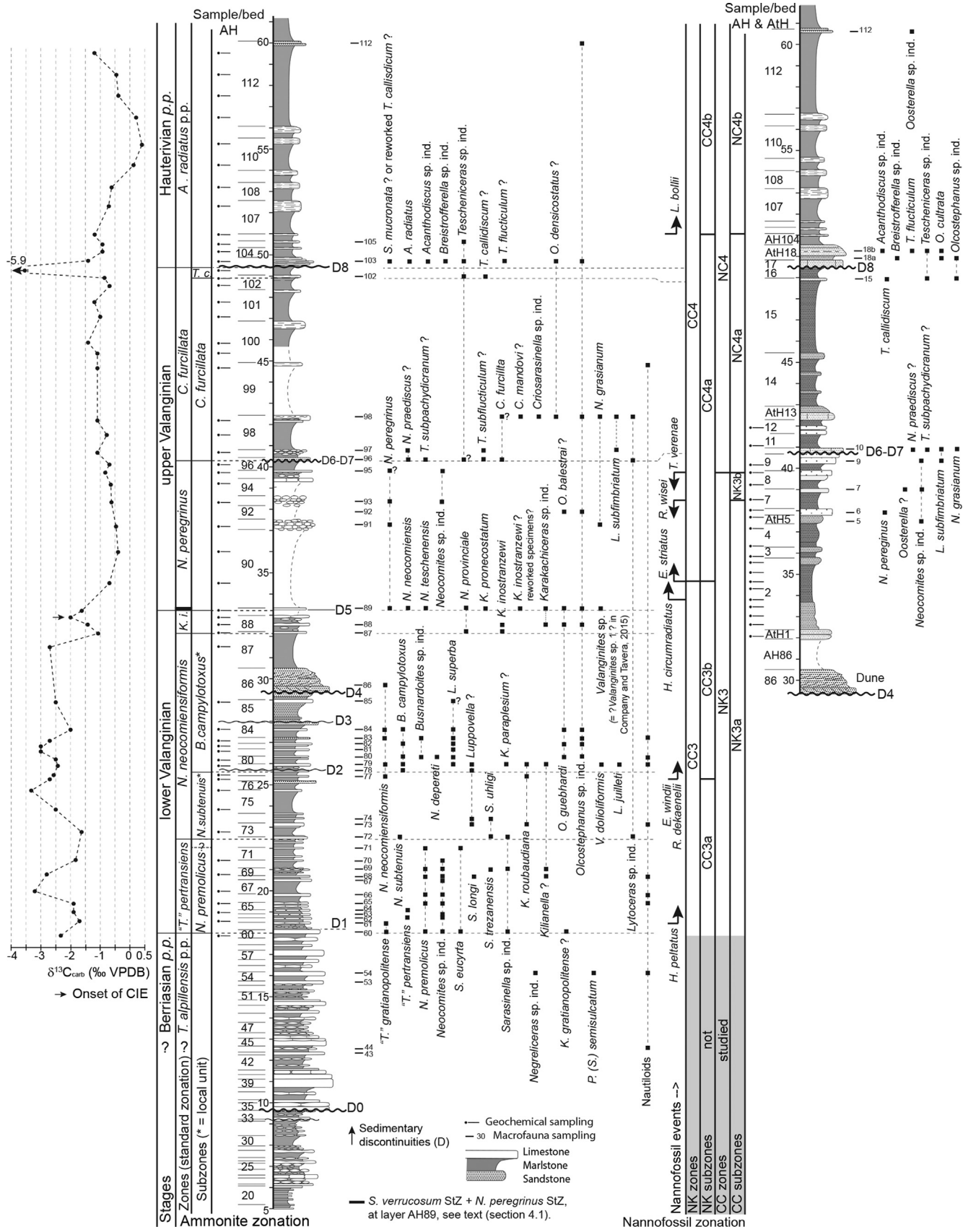

Fig. 4. The Aït Hamouch section (two outcrops). Stratigraphic distribution of macrofauna (mainly ammonites; a question mark is added when identification is doubtful) and ammonite zonation (standard and local units); layers of sampling are indicated at the right of the succession. Nannofossil zonation (NK, NC and CC) and bioevents (FO and LO) from Shmeit et al. (2022) and completed in this work. Sedimentary discontinuities (D). Carbon isotopic curve; layers of sampling are indicated at the left of the succession. The alphanumeric notation is "AH", except for the interval between 32 and 50.5 m of the right-hand column where "AtH" is used (AtH1–AtH18).

the Moroccan lower Valanginian successions. It could not be integrated in the zonal schemes of Wippich (2003) and Ettachfini (2004) as this zone was proposed by Company and Tavera (2015). This index-species is relatively rare and only found in the upper part of the zone in the Zalidou, Aït Hamouch, Igouzoulen, Ida w Iddar and Obbay sections. Consequently, the base of the zone is identified in the six studied Moroccan sections by the FO of *N. subtenuis* (Figs. 3–8, ZA25, AH72, ZS43b, IGz23, IW15b and OB18) as its appearance is contemporaneous with that of *N. neocomiensiformis* in SE Spain (Company and Tavera, 2015). In terms of stratigraphic interval, the *N. subtenuis* LSz (Ettachfini, 2004) used here corresponds to the *Baronnites hirsutus* Subzone proposed by Company and Tavera (2015). Indeed, the FO of *N. subtenuis* is simultaneous to that of *B. hirsutus* (Company and Tavera, 2015) and the upper boundary of these subzones is defined by the FAD of *B. campylotoxus* (Ettachfini, 2004) and *Valanginites dolioliformis* (Company and Tavera, 2015), respectively; according to the latter authors, the appearance of these both species is contemporaneous. It is difficult to characterize the *N. subtenuis* LSz in the Moroccan sections because the assemblage is poor and *B. hirsutus* was not identified (Wippich, 2001, 2003; Ettachfini, 2004; this work). In the *N. subtenuis* LSz, rare *Sarasinella uhligi* and/or *Karakaschiceras paraplesium* have been recorded in the Zalidou, Aït Hamouch and Igouzoulen sections (Figs. 3–4, 6). The occurrence of *S. uhligi* in the zonal scheme of Wippich (2003, fig. 10) allows to identify the *N. subtenuis* LSz in the upper part of his "*T.*" *pertransiens* StZ. In the same interval, specimens identified by Wippich (2001, 2003) as *N. neocomiensis* may be partly interpreted as *N. subtenuis*. The range of *K. paraplesium* is concordant with that observed in SE Spain (mainly in the *B. hirsutus* Subzone of Company and Tavera, 2015, fig. 7). In the Aït Hamouch and Ida w Iddar sections (Figs. 4, 7), *Kilianella roubaudiana* is recorded in the *N. subtenuis* LSz. Some specimens identified with doubt to *Luppovella* were observed in the lower part of the *N. subtenuis* LSz in the Aït Hamouch section (Fig. 4). This agrees with the data of Ettachfini (2004) as this author observed the appearance of this genus at the base of this subzone. However, contrary to the observation made in SE Spain by Company and Tavera (2015, fig. 7), *Luppovella superba* has never been recorded in the upper part of the "*T.*" *pertransiens* StZ of the Moroccan series (Wippich, 2001, 2003; Ettachfini, 2004; this work). This is in agreement with Kenjo (2014) and Kenjo et al. (2021), who noted in SE France the FO of *L. superba* in the *N. neocomiensiformis* StZ (see also Bulot (1995), who indicated this event in his *Olcostephanus stephanophorus* Zone). In the upper part of the *N. neocomiensiformis* StZ, the base of the *B. campylotoxus* LSz is placed at the FO of its relatively abundant index-species (Figs. 3–8, ZA29, AH78, ZS47, IGz26a, IW19 and OB21). Also, this subzone is well characterized by *L. superba* and numerous *Olcostephanus guebhardi* (first acme of this olcostephanid; Zalidou, Aït Hamouch, Zaouia Sidi Abderahmane, Igouzoulen and Ida w Iddar, Figs. 3–7). This assemblage is observed by Wippich (2001, 2003) and Ettachfini (2004). In agreement with these authors, the last occurrences of *Luppovella* and/or *Kilianella* are recorded in this subzone, as well illustrated in the Aït Hamouch, Igouzoulen and Ida w Iddar sections (Figs. 4, 6–7). *Busnardoites subcampylotoxus*?, *Neohoploceras depereti* and *Lytoceras juilleti* were recorded (only one specimen for each species) in the Zalidou and Aït Hamouch sections (Figs. 3–4). The *B. campylotoxus* LSz corresponds, in terms of stratigraphic interval, to the *V. dolioliformis* Subzone of Company and Tavera (2015). Indeed, according to these authors, the FOs of both index-species are simultaneous and the upper limit of these subzones is defined by the FO of *Karakaschiceras inostranzewi* (see also Ettachfini, 2004; this work). However, *V. dolioliformis* is only recorded in the *B. campylotoxus* LSz of the Aït Hamouch and Igouzoulen sections (Figs. 4, 6).

The *Karakaschiceras inostranzewi* Standard Zone. The base of this zone is placed at the FO of its index-species (Figs. 3–8, ZA34a, AH87, ZS50, IGz27a, IW26 and OB22). The *K. inostranzewi* StZ corresponds to the *Karakaschiceras biassalense* Zone of Wippich (2001, 2003) and Ettachfini (2004). According to these authors, the fauna of this stratigraphic interval is little diversified. Among neocomitids, the FO of *Neocomites neocomiensis*, *Neocomites teschenensis* and *Neocomites platycostatus* are recorded in this zone at Zalidou and Obbay (Figs. 3, 8). Few *Neohoploceras* (FO of *Neohoploceras provinciale*; Aït Hamouch, Ida w Iddar and Obbay sections, Figs. 4, 7–8) are also represented. Bulot and Thieuloy (1995), Company and Tavera (2015) and Aguado et al. (2018) also recorded the FO of *N. provinciale* in the basal part of the *K. inostranzewi* StZ. Specimens of *O. guebhardi* (beginning of the second acme) were found in most sections (Figs. 3–5, 8).

The *Saynoceras verrucosum* Standard Zone; the *S. verrucosum* and *Karakaschiceras pronecostatum* Standard subzones – Base of the upper Valanginian substage. Wippich (2003) and Ettachfini (2004) emphasized the difficulty to identify the base of the *S. verrucosum* StZ due to the scarcity of the index-species in the Moroccan successions. For example, only a single specimen was found by Wippich (2001, 2003; Tarourirt Oubazine section). Moreover, as noted by this author, the succession is highly condensed and the thickness is much reduced around the lower (*K. inostranzewi* StZ)–upper (*S. verrucosum* StZ) Valanginian boundary (see also this work). As the identification of this boundary is problematic in the western High Atlas, Ettachfini (2004) chosed to place the base of the upper Valanginian at the base of his *K. biassalense* Zone, as suggested by Bulot and Thieuloy (1995) at the base of their *K. inostranzewi* Zone in SE France. Even though no specimen of *S. verrucosum* was found in the six studied Moroccan sections (Figs. 3–8), this suggestion was not followed here to agree with the standard zonation and its chronostratigraphic subdivisions (Reboulet et al., 2018). In absence of *S. verrucosum*, the (base of the?) *S. verrucosum* StZ is identified by the (first) occurrence of *Valanginites ventrotuberculatus* as recorded in the Zaouia Sidi Abderahmane (ZS52), the Igouzoulen (IGz27c), and Obbay (OB24) sections (Figs. 5–6, 8). Indeed, according to Company and Tavera (2015), the FOs of both these species are simultaneous in SE Spain; their range ends in the basal part of the *S. verrucosum* StZ and they do not co-occur with *K. pronecostatum* (Aguado et al., 2018), index-species of the second subzone of the *S. verrucosum* StZ. In the Zaouia Sidi Abderahmane and Obbay sections, *V. ventrotuberculatus* is found with *K. pronecostatum*. In the latter section, *Saynoceras contestatum* is also recorded together with *K. pronecostatum* (OB24), as shown in Ettachfini (2004, see tab. 5, p. 82). However their ranges do not overlap in SE France (Bulot and Thieuloy, 1995) and SE Spain (Aguado et al., 2018). As *K. pronecostatum* appears in the upper part of the zone, its co-occurrence with *S. contestatum* and *V. ventrotuberculatus* in some Moroccan sections may be explained by a condensed lithology in the basal part of the upper Valanginian (see above; this work), even though a mistake in the identication of these specimens of *Karakaschiceras* cannot be excluded. For Ettachfini (2004), the base of the *S. verrucosum* StZ is characterized by the FO of *O. guebhardi* morphe *querolensis* that is well represented in the lower part of his *S. verrucosum* horizon. This may correspond, at least partly, to the second acme of *O. guebhardi*, as observed at Zalidou, Igouzoulen, and Ida w Iddar (Figs. 3, 6–7). In Zalidou and Ida w Iddar sections, the base or the lower part of the *S. verrucosum* StZ is not well identified due to the absence of ammonite markers (*V. ventrotuberculatus* and *S. contestatum*). Thus, the second acme of *O. guebhardi* might be used to approximate the lower–upper Valanginian boundary; in this case, it could be put at the base of layers ZA36 (Fig. 3; boundary indicated by a dashed line) and IW29

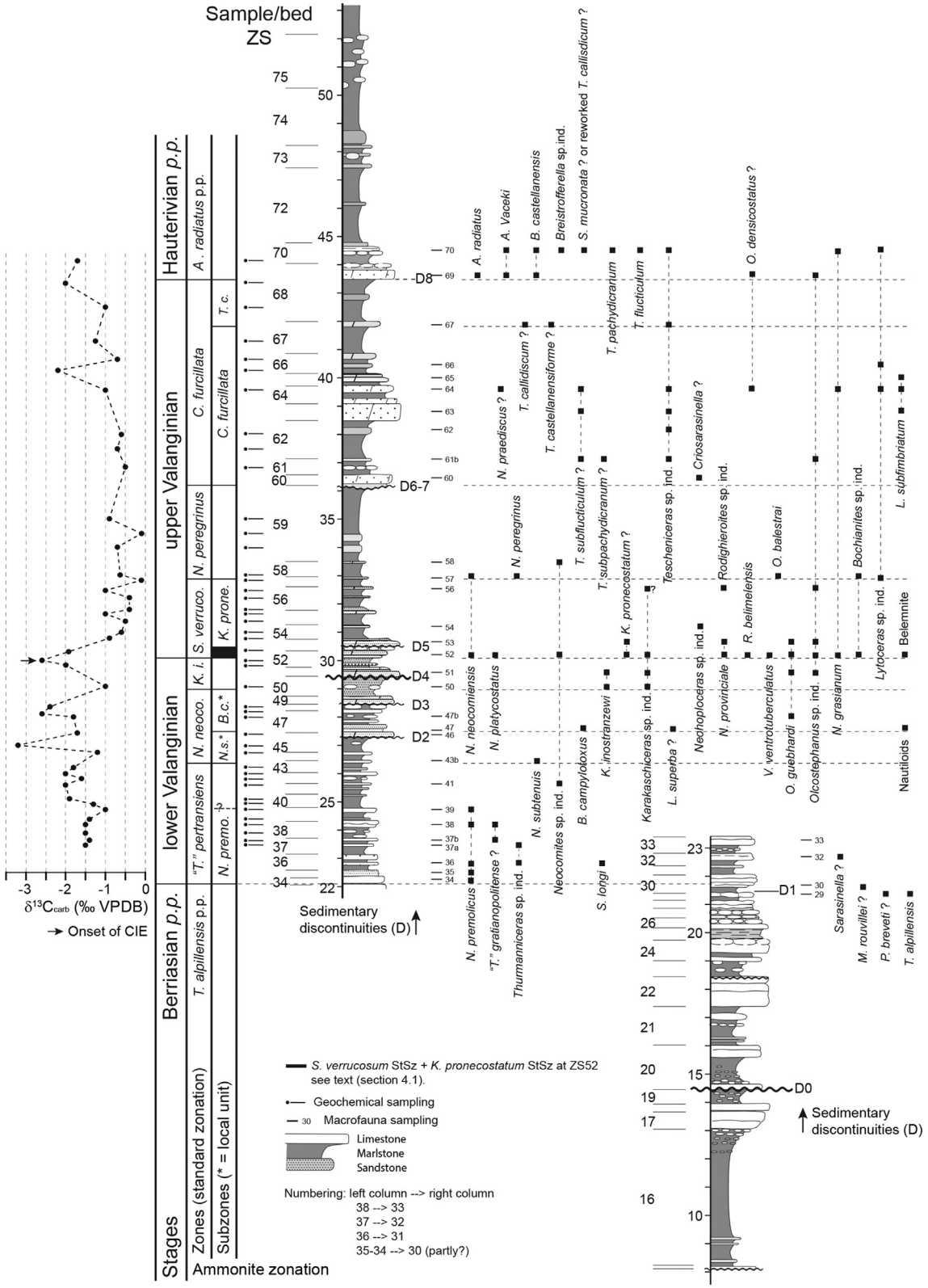

Fig. 5. The Zaouia Sidi Abderahmane section (two outcrops). Stratigraphic distribution of macrofauna (mainly ammonites; a question mark is added when identification is doubtful) and ammonite zonation (standard and local units); layers of sampling are indicated at the right of the succession. Sedimentary discontinuities (D). Carbon isotopic curve; layers of sampling are indicated at the left of the succession.

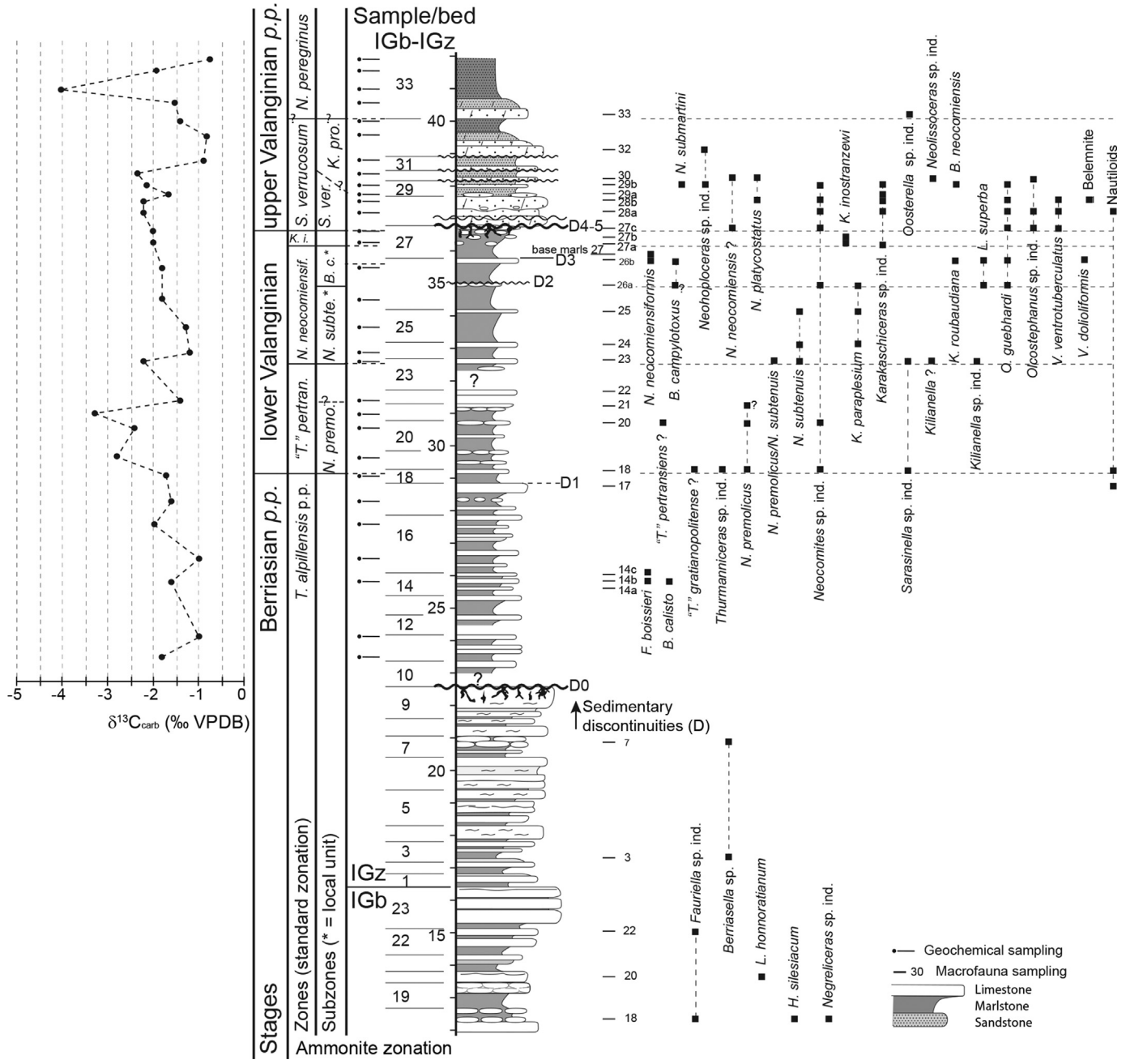

Fig. 6. The Igouzoulen section. Stratigraphic distribution of macrofauna (mainly ammonites; a question mark is added when identification is doubtful) and ammonite zonation (standard and local units); layers of sampling are indicated at the right of the succession. Sedimentary discontinuities (D). Carbon isotopic curve; layers of sampling are indicated at the left of the succession. The alphanumeric notation is "IGz", except in the basal part of the section (between 12 and 16.3 m) where "IGb" is used.

(Fig. 7). This solution is applied for the latter section, in which typical ammonite markers of the lower part of the upper Valanginian are absent. In the Zalidou section, however, the FO of *K. pronecostatum* (ZA40, boundary indicated by a solid line) is used to place the base of the zone. According to Wippich (2003), *N. platycostatus* is restricted to the *S. verrucosum* StZ, as observed in the Zaouia Sidi Abderahmane and Igouzoulen sections (Figs. 5–6). However, this neocomitid is already present in the upper part of the *K. inostranzewi* StZ in the Obbay section (Fig. 8); similar observations were made in SE France (Reboulet, 1996; Reboulet and Atrops, 1999; in their *N. platycostatus* Horizon) and SE Spain (Company and Tavera, 2015; in their *S. contestatum* Subzone). Ettachfini (2004), who considered that *N. platycostatus* is a junior synonym of *N. teschenensis*, indicated the FO of this species at the base of the *K. inostranzewi* StZ. If the (base of the) *S. verrucosum* StZ cannot be identified by the FO of *N. platycostatus*, the latter species seems (more) abundant in this zone, as observed in the Zaouia Sidi Abderahmane and Obbay sections (Figs. 5, 8). It can be expected that the distribution of *N. platycostatus* recorded by Wippich (2003) only corresponds to the highest frequency of this species in the *S. verrucosum* StZ. As *Neocomites* gr. *platycostatus–teschenensis* are relatively well represented in layers ZA36–37 (Fig. 3), this interval of the Zalidou section could be dated to this zone, as previously evoked based on the abundance of *O. guebhardi* (cf. 2nd acme). However, the lower boundary of this zone cannot be placed using the abundance variations of some taxa that are partly controlled by

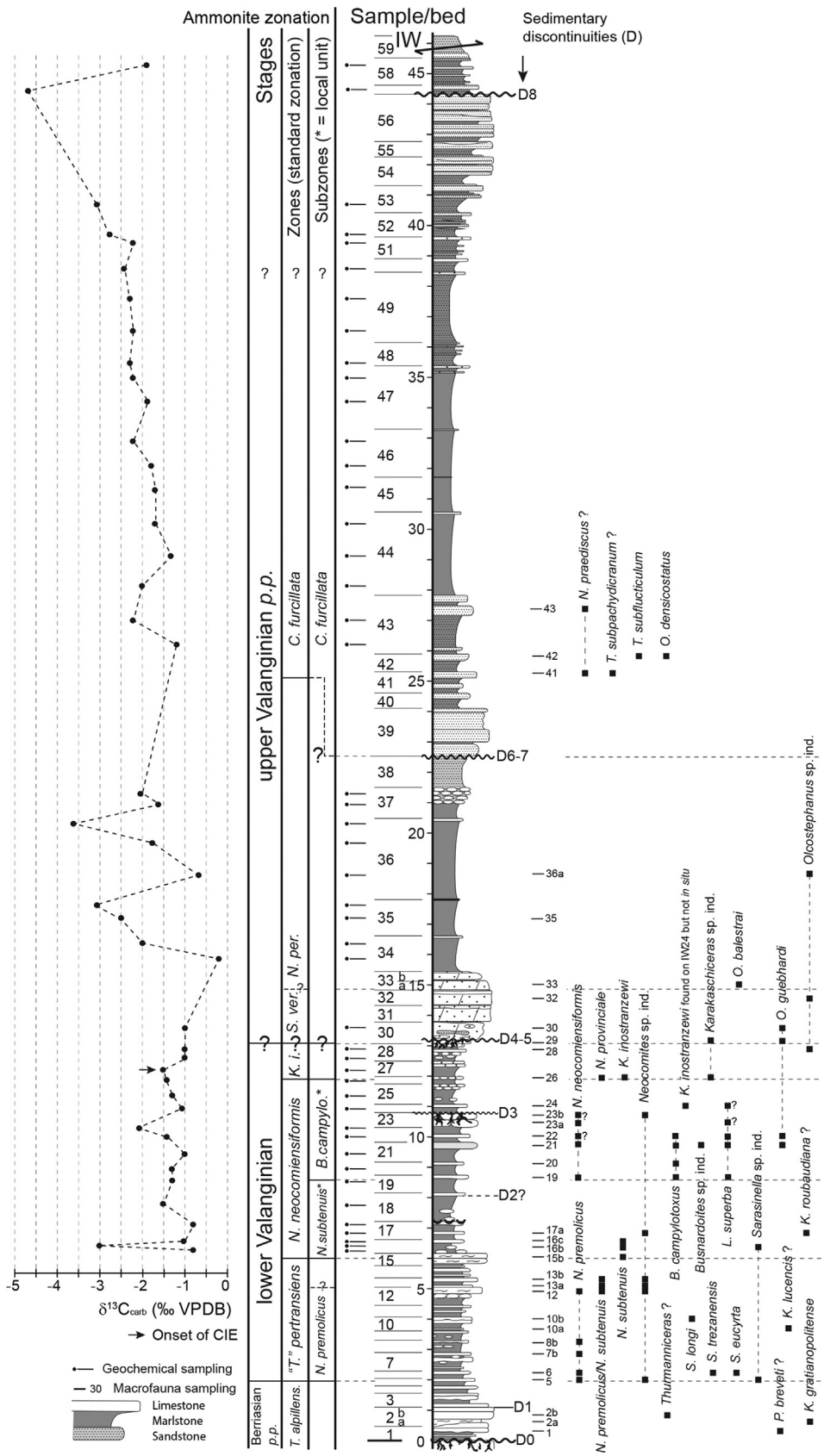

Fig. 7. The Ida w Iddar section. Stratigraphic distribution of macrofauna (mainly ammonites; a question mark is added when identification is doubtful) and ammonite zonation (standard and local units); layers of sampling are indicated at the right of the succession. Sedimentary discontinuities (D). Carbon isotopic curve; layers of sampling are indicated at the left of the succession.

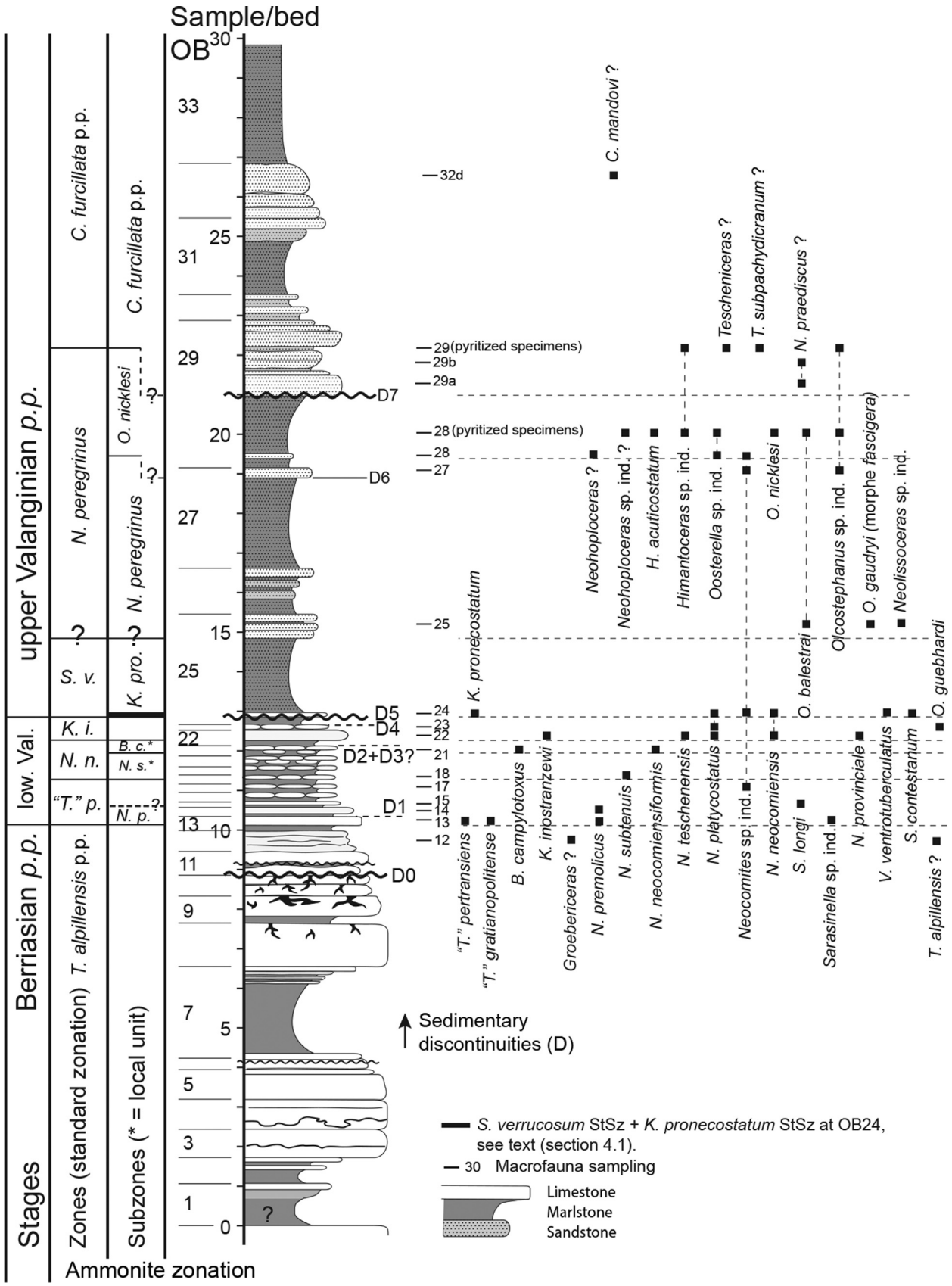

Fig. 8. The Obbay section. Stratigraphic distribution of macrofauna (mainly ammonites; a question mark is added when identification is doubtful) and ammonite zonation (standard and local units); layers of sampling are indicated at the right of the succession. Sedimentary discontinuities (D).

palaeoenvironmental conditions (see Reboulet et al., 2003) and sedimentary factors (cf. condensed layers). At Zaouia Sidi Abderahmane (Fig. 5), one specimen of *Rodighieroites belimelensis* is recorded in the *S. verrucosum* StZ; this is in agreement with Wippich's data (2003; in *K. pronecostatum* StSz). In the Igouzoulen section (Fig. 6), *Neohoploceras submartini* occurs in the *S. verrucosum* StZ; Ettachfini (2004) also observed this distribution. Taking into account that the LO of *N. submartini* is recorded in the basal part of the *K. pronecostatum* StSz in SE Spain (Aguado et al., 2018), the base of this subzone in the Igouzoulen section could be placed around the layer IGz29b. However, this should be interpreted carefully as the ranges of *Neohoploceras* taxa show some discrepancies (see Bulot and Thieuloy, 1995; Reboulet, 1996; Wippich, 2001, 2003; Ettachfini, 2004; Aguado et al., 2018); the same remark can be done for the distribution of *Rodighieroites* taxa. In two Moroccan sections, *N. provinciale* occurs in the lower part of the upper Valanginian. At Zaouia Sidi Abderahmane, this species co-occurs with *K. pronecostatum* in the basal part of the *S. verrucosum* StZ (Fig. 5, ZS52–53). According to Bulot and Thieuloy (1995) and Ettachfini (2004), *K. pronecostatum* seems to appear just after the disappearance of *N. provinciale*. Thus, as evoked previously, this Moroccan ammonite assemblage may be interpreted as a result of a condensed lithology and/or a misidentification of some specimens because of the poor preservation of upper Valanginian ammonites. A similar interpretation is made for the Aït Hamouch section, where *N. provinciale* and *K. pronecostatum* also co-occur in layer AH89, with the record of *Neocomites peregrinus* and *K. inostranzewi*? (Fig. 4). According to Ettachfini (2004) and Aguado et al. (2018), *K. pronecostatum* and *N. peregrinus* do not co-occur but the ranges given by Bulot and Thieuloy (1995) and Reboulet and Atrops (1999) show a short overlap of both species. Even though there are some discrepancies in the distributions of *Neohoploceras* taxa (see references above), it seems that *N. provinciale* never occurs with *N. peregrinus.* The layer AH89 is also characterized by the occurrence of few dubious specimens of *K. inostranzewi*?; their preservation might indicate that they have been reworked (cf. discontinuity D5; Fig. 4). To summarize, in most of the studied Moroccan sections, it is difficult to recognized clearly the lower subzone of the *S. verrucosum* StZ (and so its base) due to: a) the absence of the index-species and the rarity of some second ammonite markers as *V. ventrotuberculatus*; b) the condensed lithology and the possibility of reworking material related to the discontinuity D5.

The *Neocomites peregrinus* Standard Zone; the *N. peregrinus* and *Olcostephanus nicklesi* Standard subzones. In the western High Atlas, this zone was identified by Wippich (2001, 2003) and Ettachfini (2004). The index-species is recorded in three sections and its FO allows to place the base of the *N. peregrinus* (Sub-)Zone in the Zalidou (ZA41), Aït Hamouch (AH89), and Zaouia Sidi Abderahmane (ZS57) sections (Figs. 3–5). However, it is relatively difficult to characterize this interval as the ammonite assemblage is poor. When the index-species is absent, the boundary between the *S. verrucosum* and *N. peregrinus* zones can be approximated using the occurrence of *Olcostephanus balestrai* and/or *Oosterella gaudryi* (or *Oosterella* sp. ind.), as made at Igouzoulen (IGz33), Ida w Iddar (IW33) and Obbay (OB25) (Figs. 6–8). The *O. nicklesi* StSz is identified in the Obbay section by the FO of the index-species (OB28). Moreover, pyritized specimens of *Himantoceras acuticostatum* were also sampled in the same layer. The occurrence of *Himantoceras* sp. ind. in the Zalidou section (ZA46, Fig. 3) allows to recognize the *O. nicklesi* StSz. Indeed, these heteromorphs are known in the basal part of this subzone (Bulot and Thieuloy, 1995; Reboulet, 1996; Reboulet and Atrops, 1999; Ettachfini, 2004). According to Wippich (2003), the only record of the *O. nicklesi* StSz corresponds to reworked specimens of *O. nicklesi* and *Himantoceras trinodosum* found in a lag deposit at the base of the *Criosarasinella furcillata* StZ in the Tamri section. For this author, this subzone "falls into an erosional hiatus at least in the west" of the studied area. This author also noted that the interval between the assemblages of the *N. peregrinus* StSz and *C. furcillata* StZ is always rather thin, even in expanded sections, suggesting "a more or less significant non-sequence all over the study area".

The *Criosarasinella furcillata* Standard Zone; the *C. furcillata* and *Teschenicera callidiscum* standard subzones. The base of the *C. furcillata* StZ is defined by the FAD of the index-species but it can be identified by the FO of *Criosarasinella* (Reboulet, 1996; Reboulet and Atrops, 1999), as made for three studied sections of the present work (Figs. 3–5; FO in ZA52d, AH96 and ZS60). In the Aït Hamouch and Obbay sections (Figs. 4, 8), *Criosarasinella mandovi* was also observed. In the western High Atlas, these both species were recorded by Wippich (2001, 2003) and Ettachfini (2004). The *C. furcillata* StZ is relatively well characterized by the occurrence of *Teschenicera subflucticulum*, *Teschenicera subpachydicranum*, *Neocomites praediscus*? and/or *Olcostephanus densicostatus*. When *Criosarasinella* is absent or rare, as in the Ida w Iddar and Obbay sections (Figs. 7–8), the base of the zone can be placed using the FO of *Teschenicera* (IW41 and OB29). At Aït Hamouch, Zaouia Sidi Abderahmane and Ida w Iddar (Figs. 4–5, 7), the occurrence of *N. praediscus*? may characterize the C. *furcillata* StSz (for the range of these latter taxa, see Reboulet, 1996; Reboulet and Atrops, 1999). In some sections, *Lytoceras subfimbriatum* and *Neolissoceras grasianum* were also recorded; the last specimens of *Bochianites* (probably *Bochianites neocomiensis*) are found in this zone (Figs. 3–5). These three latter taxa were not observed in the lower Valanginian. The *T. callidiscum* StSz was identified in the Zalidou, Aït Hamouch and Zaouia Sidi Abderahmane sections (ZA55, AH102 and AtH15, ZS67, Figs. 3–5). In the latter section, *Teschenicera castellanensiforme* was also sampled at the base of the subzone.

The *Acanthodiscus radiatus* Standard Zone – Base of the Hauterivian stage. The base of the zone is defined by the FAD of the genus *Acanthodiscus*; this marker defines the base of the Hauterivian stage (Mutterlose et al., 2020). In the Aït Hamouch (AH103) and Zaouia Sidi Abderahmane (ZS69) sections, the FO of *A. radiatus* and/or *Acanthodiscus vaceki* is used to place the lower boundary of the Hauterivian (Figs. 4–5). Where these species are absent, the FO *Breistrofferella castellanensis* has been considered in the Zalidou (ZA56) and Aït Hamouch (AtH17) sections (Figs. 3–4). In the three sections (Figs. 3–5), the occurrence of *Teschenicera flucticulum* and *Teschenicera pachydicranum* allows to characterize the zone. *Oosterella cultrata* (Aït Hamouch, AtH18) and *Olcostephanus densicostatus* complete the assemblage of the basal part of the Hauterivian in the Aït Hamouch (AH103) and Zaoui Sidi Abderahmane (ZS69) sections. In both sections, few poorly preserved ammonites were found in layers AH103 and ZS70. These specimens might correspond to *T. callidiscum*? but there is no clear evidence that they were reworked from underlying levels. Alternatively, these specimens might be identified as *Saynella mucronata*(?). This species was recorded by Wippich (2003) in the condensed Tamri section, more precisely in the first layer dated from the *A. radiatus* StZ; according to this author, this may indicate a high stratigraphic level within the zone. Thus, if the identification as *S. mucronata* is correct, it seems that only the upper part of the *A. radiatus* StZ is recorded at Ait Hamouch and Zaoui Sidi Abderahmane. However, as noted by Bulot (1995), the representatives of *Saynella* are very rare in Tethyan basins and the range of *S. mucronata* has to be clarified. Even though the *A. radiatus* StZ is partly represented, it may reach a relatively large thickness at Zaoui Sidi Abderahmane as *A. vaceki*, *B. castellanensis* and *T. flucticulum* still occur around 12 m above the Valanginian–Hauterivian boundary.

Standard zonation and chronostratigraphy. The current work confirms the reproductibility of the Valanginian standard zonation (Reboulet et al., 2018) and the interest of *N. premolicus* (index-species of the *N. premolicus* StSz) to place the base of the Valanginian when "*T.*" *pertransiens* (index-species of the "*T.*" *pertransiens* StZ) is rare or even absent. Taking in account data provided by the present study, *N. subtenuis* and *B. campylotoxus* local subzones could be introduced in the standard zonation in order to subdived the *N. neocomiensiformis* StZ; these first two species are relatively easy to identify, abundant and have a widespread palaeogeographic distribution (see references above). This point might be discussed by the Kilian Group.

4.2. Calcareous nannofossil stratigraphy

The NK3A, NK3B and NC4A subzones of Bralower et al. (1995) were identified in Zalidou and Aït Hamouch sections (Figs. 3–4). In the latter section, the NC4B Subzone was additionally identified. The CC3a, CC3b and CC4a subzones of Sissingh (1977) were identified in both sections; and the CC4b Subzone was identified only at Aït Hamouch (Shmeit et al., 2022, this work). Nannofossil markers are illustrated in Appendix E (Fig. E1, Supplementary material). Quantitative data on calcareous nannofossils is provided by Shmeit et al. (2022) and can be found online (Supplementary material at https://doi.org/10.1016/j.marmicro.2022.102134).

Detailed biostratigraphic results and interpretations are presented in the current work and not in Shmeit et al. (2022). Although *Calcicalathina oblongata* defines the base of the NK3 Zone, the precise identification of the FO of this species is problematic due to different taxonomic concepts. Its FO is considered to be situated just above the Berriasian–Valanginian boundary (lower part of the "*T.*" *pertransiens*, Duchamp-Alphonse, 2007; Kenjo et al., 2021) or in the lower Valanginian (Aguado et al., 2000). Indeed, Aguado et al. (2000) recognized earlier specimens, called *Calcicalathina praeoblongata*, which occur in the upper Berriasian (*T. alpillensis* StSz); these are very similar in morphology to *C. oblongata* but smaller in average size and with a thick wide wall. However, *C. praeoblongata* figured in Aguado et al. (2000) has been considered by other authors to be overgrown specimens of *Rhagodiscus asper* (see Kenjo et al., 2021). In the present work, small specimens of *C. oblongata* (<6 μm) with a thin and bright wall have been recognized in the first samples of the two studied sections; however, in these samples, nannofossils are characterized by large overgrowths which makes more difficult the differentiation between these small forms and larger *C. oblongata*. This species was present in both sections from the first studied sample (*T. alpillensis p.p.* StZ, Zalidou section). The LO of *Rucinolithus wisei*, marking the base of the NK3B Subzone, was observed in the lower part of the upper Valanginian in both sections (*N. peregrinus* StZ at Zalidou and Aït Hamouch, respectively; Figs. 3–4). The LO of *Tubodiscus verenae*, defining the base of the NC4 Zone, was observed in the upper part of the upper Valanginian (uppermost *O. nicklesi* StSz) at Zalidou and in the lower part of the upper Valanginian (uppermost *N. peregrinus* StZ) at Aït Hamouch. The FO of *Lithraphidites bollii*, defining the base of the NC4B Subzone, was observed only at Aït Hamouch in the lowermost Hauterivian *p.p.* (lowermost *A. radiatus p.p.* StZ). The FO of *E. windii*, which identifies the base of the CC3b Subzone, was observed in the middle part of the lower Valanginian (*N. neocomiensiformis* StZ, *N. subtenuis* LSz) at Zalidou and Aït Hamouch. The FO of *E. striatus*, identifying the base of the CC4 Zone, was observed around the lower–upper Valanginian boundary (*K. inostranzewi* StZ or *S. verrucosum* StZ according to the ammonite biostratigraphic interpretation) at Zalidou and in the lower part of the upper Valanginian (*N. peregrinus* StZ) at Aït Hamouch. The identification of *Eiffelithus striatus* followed Shmeit et al. (2022), such that coccoliths have the length of their long-axes greater than 6.0 μm and with a relatively wide central area (almost 2/3 or greater of coccolith length).

Secondary nannofossil bioevents were also observed. The FO of *Speetonia colligata* was recorded in the uppermost Berriasian *p.p.* (*T. alpillensis p.p.* StZ, lowermost NK3A and lowermost CC3a subzones) at Zalidou. It was present from the first studied sample at Aït Hamouch. The FO of *Rhagodiscus dekaenelii* was observed in the lowermost Valanginian (lower *N. premolicus* StSz, lowermost NK3A and lower CC3a subzones) at Zalidou. Its FO was recorded slightly later in Aït Hamouch, in the lower Valanginian (upper *N. subtenuis* LSz, lower NK3A Subzone and CC3a/CC3b subzones boundary). The FO of *Haqius peltatus* was observed in the lower Valanginian in both studied sections; in the upper *N. premolicus* StSz (lower NK3A and upper CC3a subzones) at Zalidou, and in the lower *N. premolicus* StSz (lower NK3A and lower CC3a subzones) at Aït Hamouch.

At Zalidou, the LO of *R. wisei* is observed in the early upper Valanginian (*N. peregrinus* StZ, *N. peregrinus* StSz, lower CC4a calcareous nannofossil Subzone), and the LO of *T. verenae* is recorded in the uppermost Valanginian (*N. peregrinus* StZ, *O. nicklesi* StSz, upper CC4a Subzone). Accordingly, the NK3B Subzone extends from 22 to 34.8 m (12.8 m thickness; Fig. 3). However, at Aït Hamouch, the NK3B Subzone is considerably reduced, and extends from 38.6 to 39.8 m (1.2 m thickness, Fig. 4). Ammonite biostratigraphy provides additional information such that the *N. peregrinus* StZ is also reduced at Aït Hamouch (~7 m) compared with Zalidou (~14 m), and the *O. nicklesi* StSz is not recognized at Aït Hamouch (Figs. 3–4). Additionally, there is no lithological evidence of a condensed interval in the upper part of the *N. peregrinus* StZ, where the LOs of *R. wisei* and *T. verenae* have been recognized. This might indicate that a time-interval is missing in Aït Hamouch compared with Zalidou.

To synthetize: a sequence of seven nannofossil bioevents has been recognized in the EAB allowing an accurate biostratigraphic framework to be established. They have been correlated with the ammonite zonation. A comparison of this integrated stratigraphy (ammonites and calcareous nannofossils) with other Tethyan basins is shown in the synthetic Fig. 9, and is described as follows.

The FO of *S. colligata* is recorded in the upper Berriasian *p.p.* (*T. alpillensis* StZ). This event has the same age in other basins: the Subbetic Basin (Spain, Aguado et al., 2000), the Neuquén Basin (Argentina; Bown and Concheyro, 2004), the site 1213 (Shatskey rise, Pacific Ocean; Bralower et al., 2002) and the southern Carpathians (Romania; Melinte and Mutterlose, 2001).

The FO of *H. peltatus* is recorded in the lowermost Valanginian ("*T.*" *pertransiens* StZ, *N. premolicus* StSz). In site 1213 (Shatskey rise, Pacific Ocean), this species first occurs in the lower Berriasian (Bralower et al., 2002), i.e. earlier than in the EAB. In the Subbetic Basin, the range of *H. peltatus* starts in the latest lower Valanginian (*K. inostranzewi* StZ, *N. platycostatus* StSz; Aguado et al., 2018); it should be noted that their sampling only concerns the upper part of the *N. neocomiensiformis* StZ and the *K. inostranzewi* StZ. The differences in the FO of *H. peltatus* may be partly explained by its sporadic distribution, as it has been observed in the Valanginian of the EAB.

The FO of *E. windii* is recorded in the lower Valanginian (*N. neocomiensiformis* StZ). This is in accordance with observations of Duchamp-Alphonse et al. (2007) in the Vocontian Basin (SE France, Angles section). In this basin, Bergen (1994) recorded this event slightly later, whereas Kenjo et al. (2021) observed the FO of *E. windii* in the lower part of the "*T*". *pertransiens* StZ. In other basins, the first record of this species is also dated as lower Valanginian: DSDP 535 (Gulf of Mexico; Bergen, 1994), site 1213 (Shatskey rise, Pacific Ocean; Bralower et al., 2002), Neuquén Basin (Argentina; Bown and Concheyro, 2004) and BGS hole 81/43 (southern North Sea; Kessels et al., 2006).

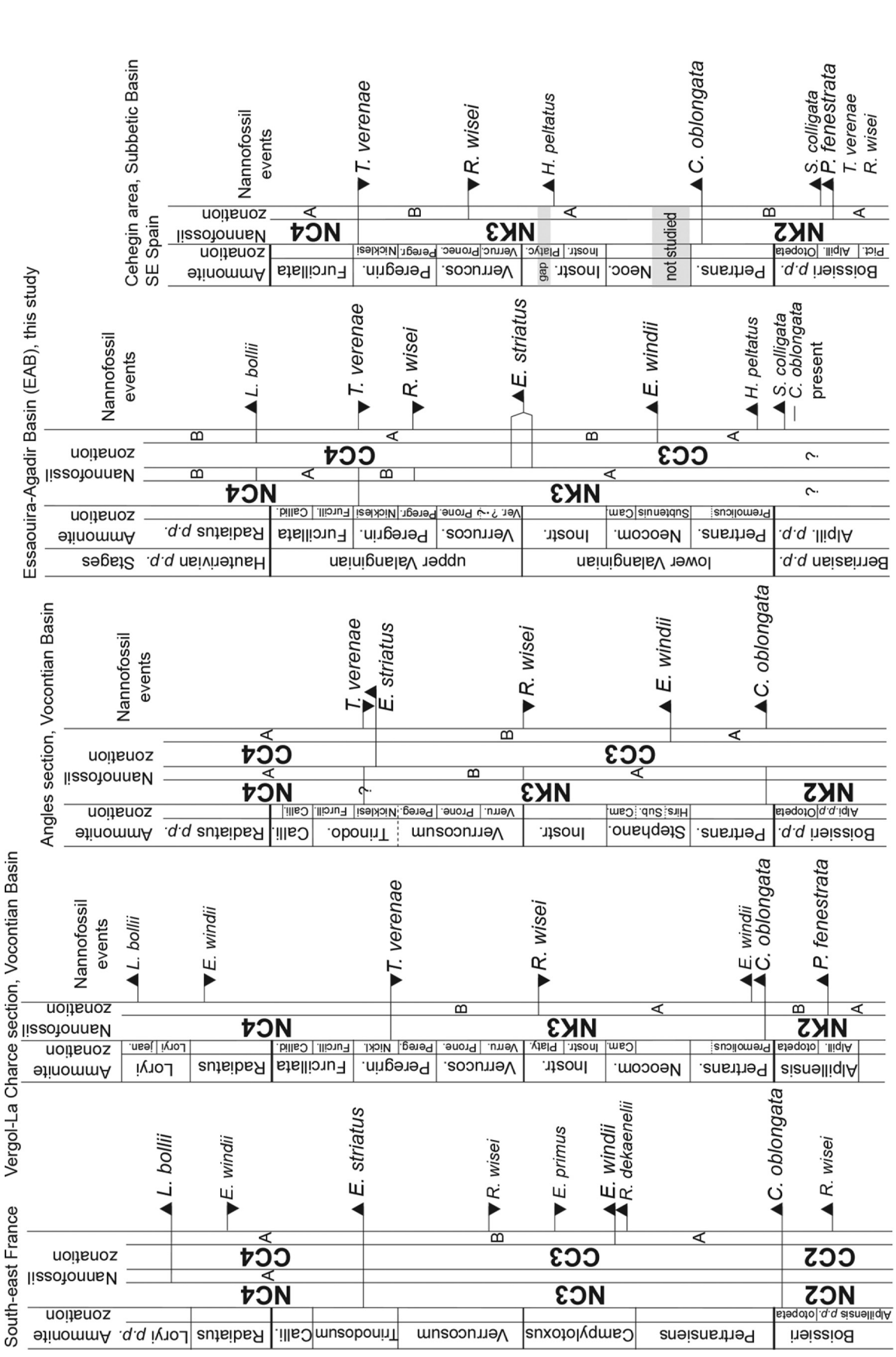

Fig. 9. Calcareous nannofossil events and zonation calibrated with the ammonite standard zonation of the Essaouira-Agadir Basin (this study) and their comparisons with existing Tethyan biozonal schemes where both ammonite and nannofossil records are also available: South–east France modified from Bergen (1994); Vergol-La Charce composite section (Vocontian Basin) modified after Gréselle et al. (2011), Mutterlose et al. (2020) and Kenjo et al. (2021); Angles section (Vocontian Basin) modified after Duchamp-Alphonse et al. (2007); Cehingin area (Subbetic Basin, SE Spain) modified after Aguado et al. (2000, 2018). The FO of *E. striatus* is situated in the *K. inostranzewi* StZ or *S. verrucosum* StZ according to the ammonite biostratigraphic interpretation of the Zalidou section (see Section 4.1).

The FO of *E. striatus* is recorded around the lower–upper Valanginian boundary. The age of this event varies according to the geographic locations of the studied sections. It is considered upper Valanginian (former *H. trinodosum* Zone) in the Vocontian Basin (Bergen, 1994; Duchamp-Alphonse et al., 2007), or in the Neuquén Basin (*N. peregrinus* StZ; Bown and Concheyro, 2004), whereas it is uppermost Valanginian in the Boreal Realm (Greenland–Norwegian Seaway; Möller et al., 2015). Moreover, Kessels et al. (2006) recorded the FO of *E. striatus* in the uppermost Valanginian along a N–S transect (BGS hole 81/43 – southern North Sea, DSDP 638 – northern west Spain and DSDP 535 – western Atlantic). Aguado et al. (2018) already suggested that the distribution of *E. striatus* might be controlled by the palaeogeographic distribution of land masses and by the palaeoceanographic currents.

The LO of *R. wisei* is recorded in the upper Valanginian (*N. peregrinus* StZ). In the Subbetic Basin (SE Spain; Aguado et al., 2018), its LO is recorded in the upper Valanginian, but slightly earlier (*S. verrucosum* StZ) than in the EAB. In the Vocontian Basin, its LO is recorded earlier, at the lower–upper Valanginian transition (Bergen, 1994; Duchamp-Alphonse et al., 2007; Gréselle et al., 2011). Discrepancies in the LO of *R. wisei* may be explained by its scarcity at the top of its range (Aguado et al., 2018).

The LO of *T. verenae* is recorded in the upper Valanginian (*N. peregrinus* StZ, *O. nicklesi* StSz). This bioevent is also observed in a similar stratigraphic interval (*O. nicklesi* StSz) both in the Vocontian Basin (Duchamp-Alphonse et al., 2007; Gréselle et al., 2011) and in the Subbetic Basin (Aguado et al., 2018).

The FO of *L. bollii* is recorded in the lowermost Hauterivian (*A. radiatus* StZ). This event is observed later (*Crioceratites loryi* StZ) in the Vocontian Basin (Duchamp-Alphonse et al., 2007; Mutterlose et al., 2020) than in the EAB.

Among these seven bioevents, three appear synchronous and are reliable for inter-basin correlation: the FOs of *S. colligata* and *E. windii*, and the LO of *T. verenae*.

4.3. Sedimentology and sequence stratigraphy

4.3.1. Sedimentary discontinuities (Figs. 10–11)

Karst. The top of massive limestone beds frequently presents cm-to dm-scale cavities infilled by marly sediment, distinct from the surrounding limestone, that may contain lithoclasts. When the section is visible, cavities usually decrease in size downward and show a random shape. Fossils in the beds may be dissolved and replaced by iron-rich calcite or dolomite. These features are interpreted to result from emergence periods, which caused dissolution and karstification by meteoric water. Moreover, karstified surfaces are locally bored; boring resulted probably from the activity of lithophagous molluscs of intertidal to very shallow environment, during the subsequent marine transgression.

Corrugated surface. These surfaces are mainly marked by a wavy shape and by reworking of intraclasts in the immediately overlying bed. In the Valanginian succession, they are often observed at the base of thick beds of fine-grained sandstone or of sandy limestone, and also between thin limestone beds and are only marked by the reworking of small-sized intraclasts. These surfaces are interpreted as resulting from the erosion of the underlying bed(s) that can be reworked in the overlying deposits. In the absence of emergence evidence, they are tentatively ascribed to mainly submarine erosion periods.

Limestone to marlstone abrupt lithological change. In the lower part of the studied series, this kind of surface is usually observed at the top of limestone beds and below a marly succession. It is frequently marked with a phosphate enrichment of the limestone bed in the Berriasian units, and is locally associated with a hardground capping the latter. It is interpreted as traducing a sedimentary hiatus that allowed mineralization (P, Fe) of the bed surface.

Marlstone to sandstone abrupt lithological change. In the upper Valanginian–lowermost Hauterivian part of the series, lithological change commonly occurs between underlying marlstone and overlying thick beds of sandstone. In this case, it is interpreted as an erosional surface which allowed sandy particles to be loosened from the underlying strata, and then sorted out and deposited in a shallow marine, moderately energetic environment as deposition resumed. Usually, the importance of erosion and the occurrence of emergence periods cannot be assessed. In one case, however, the lack of biostratigraphic bio(sub-)zones suggests significant erosions during a long-lasting period of subaerial erosion.

In the following text, sedimentary discontinuities are labelled from D0 to D8 in stratigraphical order.

4.3.2. Overview of the Berriasian carbonate shelf sedimentation (Figs. 10–12)

Only the top of this series is dated as upper Berriasian (*T. alpillensis* StZ). Identification of the sedimentary discontinuities allows to recognize two depositional sequences. Although poorly dated, they are tentatively correlated across the studied sections. The far bases of the successions are not illustrated in Figs. 10 and 11 but their petrographic content is described below in order to show the sequential evolution. In the southern sections (Aït Hamouch, Sidi Abderhamane, Zalidou), the base of the succession is made of relatively massive limestone beds with thin marlstone interbeds. There, the presence of thick marlstone interbeds and an open marine fauna (plicatulids, terebratulids, large bivalves) would indicate an outer shelf environment. However, the abundance of oysters and shallow-water sedimentary features (laminations, HCS, epikarsts) rather suggests a shallow, open marine depositional environment. In the northern sections (Igouzoulen, Obbay), this succession seems to correlate with massive limestone beds made of pelloid-rich wackestone to packstone, rich in oysters, pinnids and locally oolites. The occurrence of several karstified surfaces, tidal laminations and local desiccation breccias indicates a very shallow, inner shelf environment.

The first sequence (Be1) is represented by a marly interval in the southern sections. Its base is marked by an abrupt lithological change, and by accumulations of phosphate and intraclasts. It shows a thinning-, then thickening-upward evolution. Marlstone contain brachiopods, pectinids, other bivalves among which *Trichites* sp., echinoids, serpulids, and locally bryozoans, and belemnites, whereas the bioturbated limestone beds present oysters, pinnids, and locally trigonids. Microfacies analysis of limestone beds reveals wackestone textures rich in echinoids and small benthic foraminifers, among which few agglutinated foraminifers, associated with bivalves as oysters, brachiopods and ostracods. This sequence is interpreted as a transgressive then prograding succession, in an open marine outer to inner shelf environment, and witnessing a sea level rise with respect to the underlying deposits. In the Igouzoulen section, this sequence overlies a karstified surface and is dominated by massive limestone beds with thinner marlstone interbeds. In the lower part, pinnids, echinoids, terebratulids and serpulids dominate. In the upper part, thick shelled oysters are dominant, associated with echinoids, pectinids, terebratulids, plicatulids, and finally few ammonites, trigonids and wood fragments. In thin sections, wackestone to packstone textures are predominant and contain a rich fauna of benthic foraminifers, among which are agglutinated forms. The uppermost limestone bed is deeply karstified. In the Obbay section, the upper part of the sequence is made of massive limestone beds containing oysters, trigonids and *Trichites* sp., and is affected by repeated karstification.

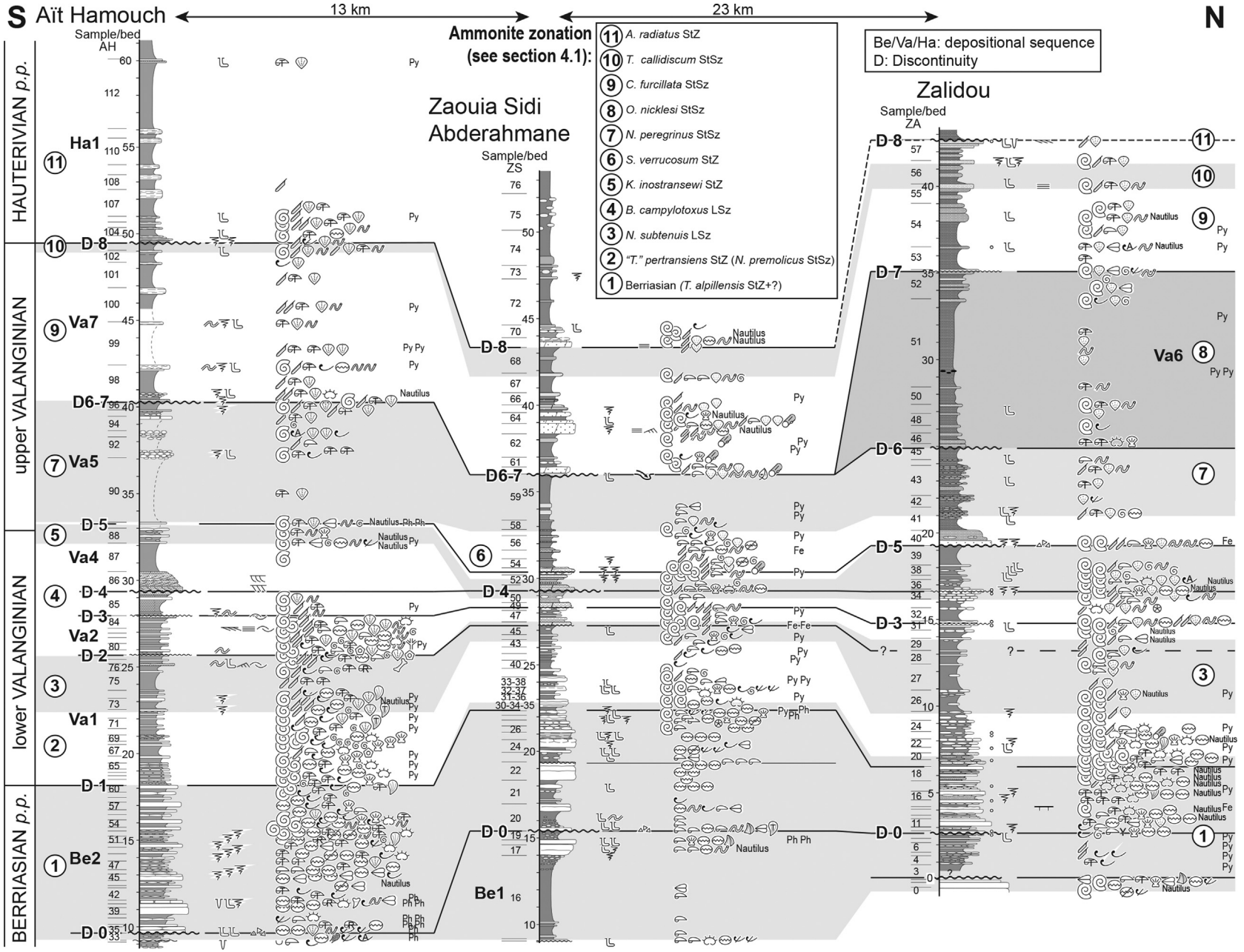

Fig. 10. Sedimentology, sequence stratigraphy and correlations (south–north transect) of Aït Hamouch, Zaouia Sidi Abderahmane and Zalidou sections from the southern part of the studied area. Caption on Fig. 11. Location on Fig. 1B.

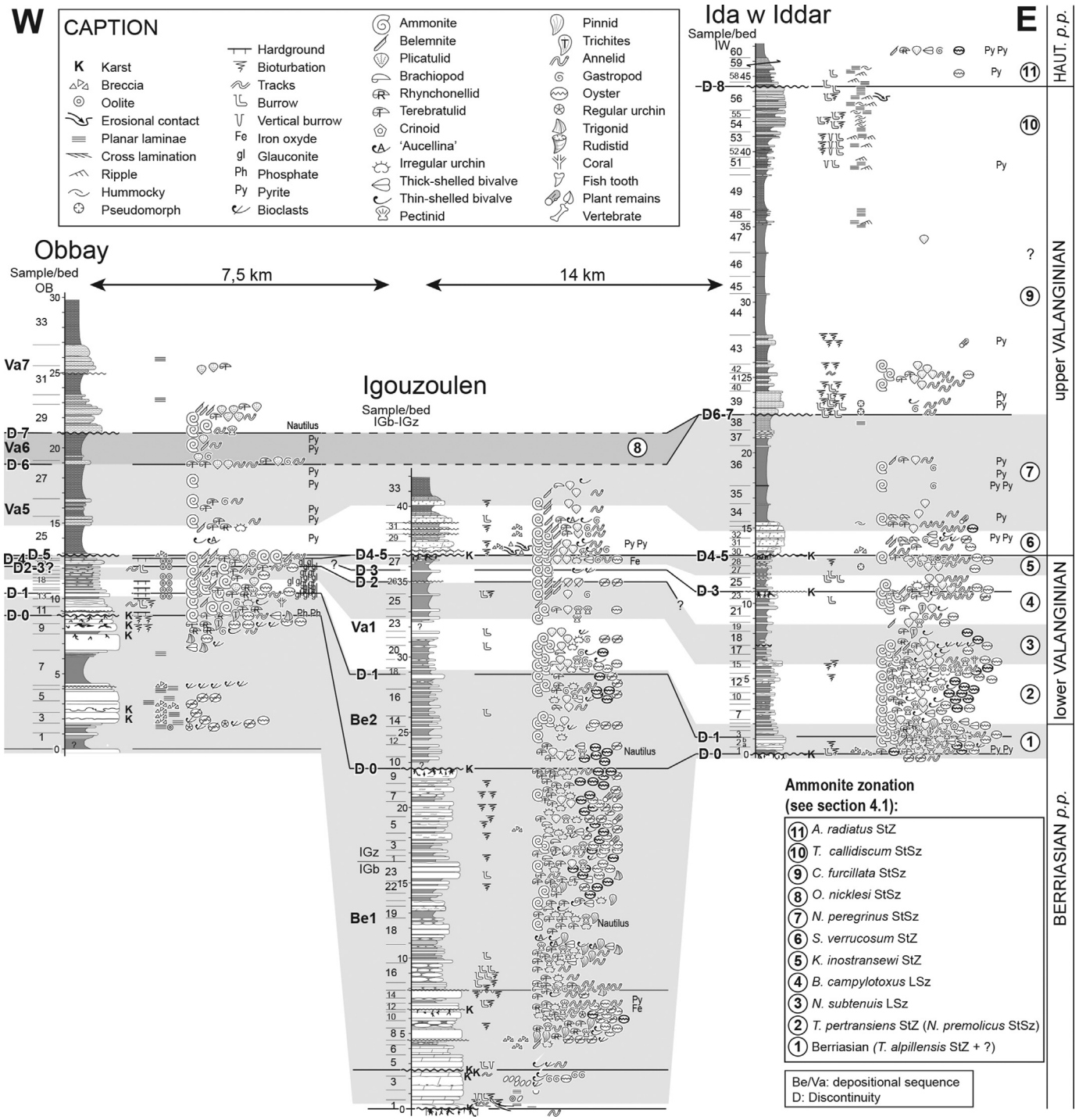

Fig. 11. Sedimentology, sequence stratigraphy and correlations (west–east transect) of Obbay, Igouzoulen and Ida w Iddar sections from the northern part of the studied area. Location on Fig. 1B.

The second sequence (Be2) consists of alternating limestone beds and marlstone interbeds; its upper part is dated as uppermost Berriasian (*T. alpillensis* StZ). Its base (D0) is an erosional surface in the southern sections and a karstified surface in the northern ones. In the southern sections, the lower three quarters of the sequence shows a thinning upward trend, while the upper quarter is slightly thickening upward. In the lower part, fauna is abundant and is dominated by oysters and terebratulids, associated with echinoids, pectinids, plicatulids, other bivalves, and locally *Trichites* sp. and fish teeth. In the upper part, ammonites and terebratulids are dominant, with oysters, pectinids, other bivalves, serpulids and nautiloids. The uppermost bed of the sequence is marked by the occurrence of pinnids and oyster coquina. Microfacies evolve from base to top, from sandy wackestone/packstone rich in echinoid remnants and small benthic foraminifers associated with calpionellids, brachiopods and scarce bryozoans, to sandy mudstone/wackestone rich in echinoids and bivalves, with subordinate calpionellids, planktic foraminifers, brachiopods and small benthic

foraminifers. In the northern sections, the same evolution is observed, but ammonites are abundant throughout the succession, and microfacies (Igouzoulen) are dominated by wackestone rich in echinoids and benthic foraminifers, both small sized and agglutinated. The presence of agglutinated foraminifers suggests a mild oxygen depletion of the shelf (Kuhnt et al., 1996; Kender and Kaminski, 2017).

In all sections, the top of the Be2 sequence is marked by an abrupt lithological change, locally marked by a hardground (Obbay). This sequence is interpreted as constituted by a thick retrograding succession, overlain by a thin prograding unit, deposited in a shallow outer shelf environment. The two above described sequences seem to represent the Cap Tefelney Fm of Rey et al. (1986, 1988).

4.3.3. Valanginian–lowermost Hauterivian mixed shelf (Figs. 10–12)

As revealed before, the Berriasian–Valanginian boundary is placed immediately above the D1 discontinuity. The identification of discontinuity surfaces allowed to identify eight transgressive-regressive sequences. Because of its condensed nature, the Obbay section will be analysed separately.

The first sequence (Va1) is a marly series that comprises scattered thin beds of limestone, belonging to the "*T.*". *pertransiens* StZ and *N. subtenuis* LSz. Its top has not been clearly identified in the Zalidou, Obbay and Ida w Iddar sections. It overlies the D1 discontinuity and presents a thick, thinning upward lower part overlain by a thin, thickening upper part. The calcareous lower part of the sequence contains dominantly oysters, pectinids, echinoids and ammonites. In its middle part, predominant ammonites, belemnites, terebratulids and plicatulids, and very local *Trichites* sp. (Aït Hamouch), express a deepening of the depositional environment. Deepest deposition is reached in the most marly part of the sequence where belemnites dominate. The uppermost part of the sequence is marked by a faunal assemblage similar to that of the lower part, which indicates a shallowing trend. In Aït Hamouch, HCS and scarce vertebrate remains express a shallower environment. The top of the sequence is marked by a discreet erosional surface. In the central sections, microfacies analysis shows the predominance of mudstone to wackestone textures, and dominant echinoids and agglutinated foraminiferas in the lower and middle part of the sequence. In the upper part, wackestone textures become dominant, with abundant echinoids and bivalves, and subordinate agglutinated foraminiferas.

The second sequence (Va2) is a set of marlstone comprising thin limestone beds, ascribed to the lower part of the *B. campylotoxus* LSz. In the southern sections, its base (D2) is an erosional surface, while it has not been recognized in the Obbay and Ida w Idar sections. In Sidi Abderhamane, it shows a clear thinning-, then thickening-upward trend, whereas it shows a homogeneous trend in other sections. The fauna consists of ammonites, belemnites, brachiopods, plicatulids and other bivalves, suggesting an outer shelf depositional environment. In thin sections, a wackestone texture is observed, containing agglutinated foraminifers, brachiopods, echinoids and benthic foraminifers. This sequence is interpreted as deposited in an open marine, outershelf environment. In Aït Hamouch, the presence of abundant oysters and serpulids, together with echinoids and scarce corals indicates a shallower, and maybe a more mesotrophic environment. This is supported by the occurrence of sandy limestone beds showing cross bedding and HCS.

The third sequence (Va3) is a thin series of marlstone with thin limestone beds. Its base (D3) is an erosional surface, and ammonites ascribe to the middle part of the *B. campylotoxus* LSz. In Igouzoulen, it is reduced to a single sandy limestone bed. Where present, the lithological and faunal evolutions are comparable to that of Va2. The interpretation is, therefore, similar.

The fourth sequence (Va4) is only present in the southern sections, where it is dated to the upper part of the *B. campylotoxus* LSz and the *K. inostranzewi* StZ. In the southernmost sections, it begins with a cross-bedded sandy bed that overlies surface D4. In Zalidou, the basal bed (ZA35) is a limestone bearing oysters, ammonites and plicatulids. The overlying marlstones are rich in pelagic fauna (ammonites, locally belemnites), and are themselves overlain by limestone beds rich in benthic fauna. In Zalidou, however, no limestone beds are observed in the upper part of the sequence, which is directly overlain by a thick sandstone bed (ZA40) suggesting that the upper part of the sequences has been eroded during D5. The Va4 sequence is interpreted as a new depositional sequence, the maximum depth of deposition reaching an outer shelf environment. In the Obbay section, the Va2 to Va4 sequences are highly condensed (~2 m), and are represented by limestone beds with thin marlstone interbeds. Limestones are slightly sandy wackestone containing predominantly phosphate- and iron-rich oolites, associated with small benthic and scarce planktic foraminifers, and few echinoid or bivalve fragments. Nuclei of oolites are frequently phosphate, glauconite or pyrite granules. These features suggest alternating high energy regime leading to condensation and oolites formation, and low energy periods allowing deposition of micrite. In some beds, partial dissolution of oolites, or local packstone texture with iron-rich micrite suggest emergence periods.

The fifth sequence (Va5) is a mainly marly to sandy succession, which is present in all sections and is dated early upper Valanginian (*S. verrucosum* StZ and *N. peregrinus* StSz). Its base (D5) is either an erosional surface, or a deeply karstified surface (Igouzoulen, Ida w Iddar). This basal discontinuity is directly overlain either by thick sandy beds (mainly to the north: Zalidou, Igouzoulen, Ida w Iddar), or by marlstone. The basal sandy beds contain both pelagic and benthic fauna to the south and west (Zalidou, Igouzoulen) and only benthic fauna to the north–east. The rest of the sequence shows a thinning-upward evolution, locally overlain by a thickening-upward succession. The marly part of the sequence yields a moderately deep outer shelf fauna (few ammonites and belemnites, associated with terebratulids, serpulids and plicatulids), among which the benthic part becomes more abundant upward.

The sixth sequence (Va6) is only recognized in the Obbay and Zalidou sections. It corresponds to the *O. nicklesi* StSz of the upper Valanginian. In both sections, surface D6 is overlain by a sandstone bed, but erosion is only visible in Zalidou. At the base, the benthic fauna (plicatulids, echinoids, pectinids) indicates a shallow, open marine environment. It is overlain by silty marlstone bearing belemnites, ammonites, serpulids, with some plicatulids and terebratulids, of outer shelf environment. The middle part of the sequene is rich in pyrite (pyritized ammonites in Obbay). In Zalidou, the upper part is a thickening upward succession of silty marlstone and sandstone beds with ammonites and benthic fauna, expressing a shallowing-upward trend. In Obbay, the reduced thickness and the lack of this thickening upward succession suggest an erosion period during the overlying D7 discontinuity. This is supported by the lack of the *O. nicklesi* StSz in most sections, and suggests that major subaerial erosion occurred during discontinuity D7.

The seventh sequence (Va7) is present in all sections and its ammonite fauna indicates the uppermost Valanginian (*C. furcillata* StSz and *T. callidiscum* StSz). It consists of a mainly marly to sandy succession that overlies an erosional surface (D7). In most sections, D6 and D7 are merged. This basal discontinuity is directly overlain by a sandy bed containing an abundant open marine fauna, among which pectinids, plicatulids and echinoids indicate a shallow environment. This is supported by the local occurrence of wood and

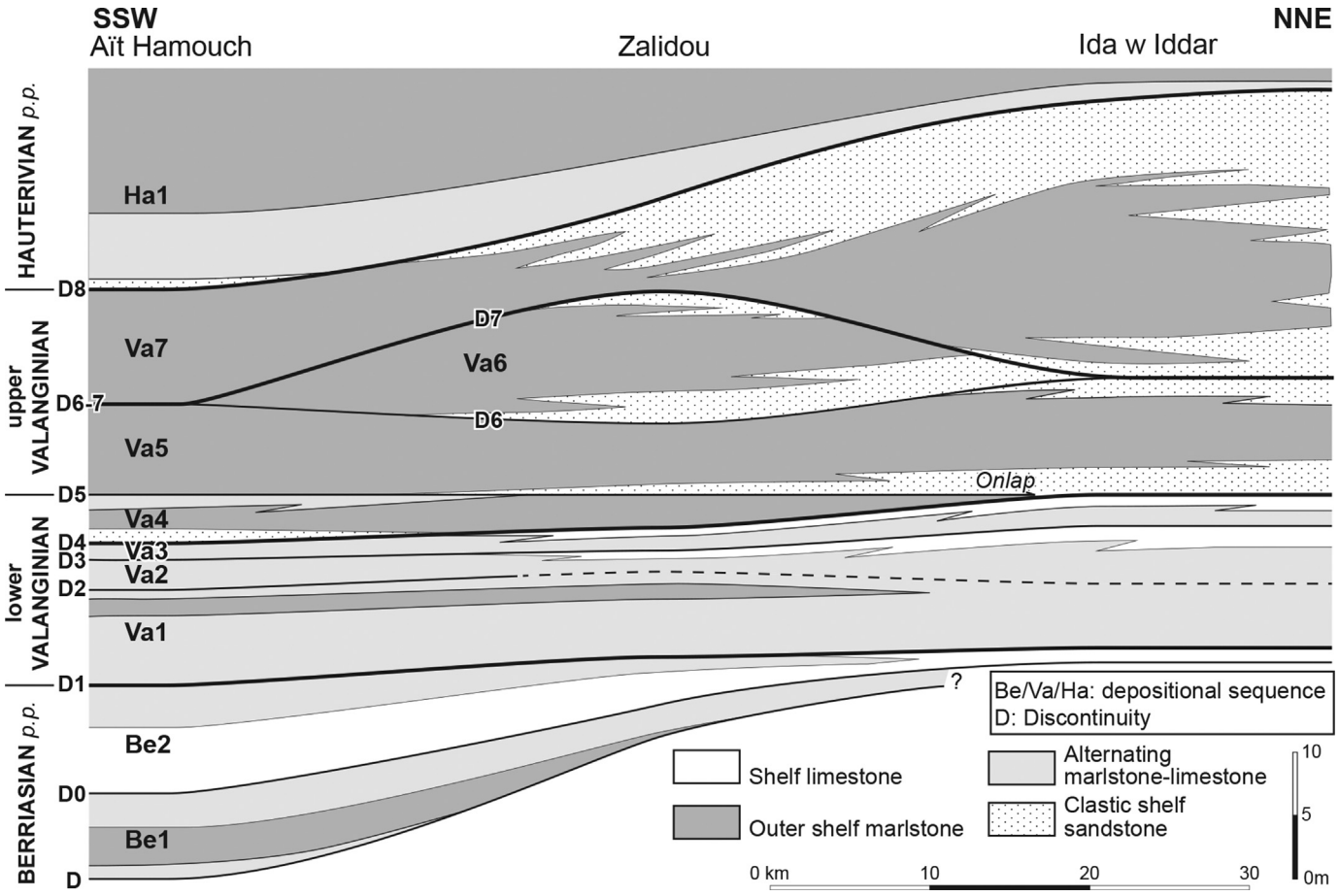

Fig. 12. Discontinuities and depositional sequences along a SSW–NNE transect including the Aït Hamouch, Zalidou and Ida w Iddar sections.

leave fragments (Sidi Abderhamane) and probable evaporite pseudomorphs (Ida w Iddar). The middle part of the sequence bears a deep outer shelf fauna (belemnites, ammonites, plicatulids, terebratulids). In the southern sections, no thickening-upward evolution is observed in the upper part of the sequence, whereas the northeastern sections (Zalidou, Ida w Iddar) display clearly the progradation of a clastic system. In the upper part of the sequence, the southern sections display an outer shelf fauna (plicatulids, belemnites, terebratulids, ammonites), while the Ida w Iddar section is marked by very shallow sedimentary features (HCS, ripple marks, tidal laminations).

Only the lower part of the eighth sequence (Ha1) has been studied. In spite of scarce ammonite fauna, discontinuity D8 seems to roughly coincide with the Valanginian–Hauterivian boundary, since ammonites of the *A. radiatus* StZ are found above (Aït Hamouch, Zaouia Sidi Abderhamane), or immediately below (Zalidou) the surface D8. Ha1 begins with a sandy bed in the southern sections (Aït Hamouch, Sidi Aberhamame), or with sandy marlstone in the northern sections. The rest of the studied succession shows a tinning-upward trend and a scarce outer shelf to pelagic fauna.

4.4. Carbon isotope stratigraphy

The measured $\delta^{13}C_{carb}$ values range between −2.8 and +1 (avg. −0.8‰) at Zalidou, −3.3 and +0.4 (avg. −1.5‰) at Aït Hamouch, −3.2 and −0.1 (avg. −1.3‰) at Zaouia Sidi Abderahmane, −4 and −0.8 (avg. −1.8‰) at Igouzoulen, and −4.7 and −0.2 (avg. −1.8‰) at Ida w Iddar (Figs. 3–7). The $\delta^{13}C_{carb}$ values of sections are provided in Appendix F (Supplementary material). Among the studied sections in the EAB, Zalidou (Fig. 3) presents the highest sampling resolution and is considered as the reference section for the $\delta^{13}C_{carb}$. The Weissert Event is identified from the base of the CIE, until its climax, following the formal definition of Erba et al. (2004). According to this definition, the CIE is observed at Zalidou from the basal part of *K. inostranzewi* StZ (16.25 m) to the upper part of *O. nicklesi* StSz, in which the climax is recorded at 32.8 m (upper NK3A to upper NK3B and upper CC3b to upper CC4a calcareous nannofossil subzones). Below this peak, there is a short-lived plateau of values comprised between 0 and 1‰ (dated from the *O. nicklesi* StSz); above the climax, the isotopic curve is characterized by a slow decrease in values (uppermost *O. nicklesi* StSz and *C. furcillata* StZ). The top of the Weissert Event is recorded just below the LO of the nannofossil biomarker *T. verenae*, marking the base of the nannofossil Zone NC4. At Aït Hamouch (Fig. 4), the CIE is cautiously identified from 32.8 (*K. inostranzewi* StZ) to ~36 m (middle part of *N. peregrinus* StZ). In this section, *S. verrucosum* StZ was not recognized separately (see AH89 and comments on ammonite biostratigraphy). Additionally, the *N. peregrinus* StZ is reduced (~7 m) compared with Zalidou (~14 m), and the *O. nicklesi* StSz was not recognized. This can be also observed from the reduced NK3B calcareous nannofossil Subzone in Aït Hamouch (1.2 m) compared with Zalidou (12.8 m). The slow decrease of $\delta^{13}C_{carb}$ values in the *C. furcillata* StZ is recorded. At Zaouia Sidi Abderahmane (Fig. 5), the CIE starts in the upper part of the *K. inostranzewi* StZ (~30 m) and the climax value is recorded in the *N. peregrinus* StZ (~34.5 m). After this peak, the decrease of the values is mainly observed in the *C. furcillata* StZ. Again, the plateau

phase of positive $\delta^{13}C_{carb}$ values is not recognized before the climax. At Igouzoulen (Fig. 6), it is difficult to recognize the CIE; it could be placed between 36 and 40 m (*K. inostranzewi* StZ and *S. verrucosum* StZ). At Ida w Iddar (Fig. 7), the CIE could be placed between 12 and 16 m (*K. inostranzewi* StZ and *N. peregrinus* StZ). It should be noted that the *C. furcillata* StZ is also characterized by a smooth decrease of $\delta^{13}C_{carb}$ values. To summarize, the plateau phase of positive $\delta^{13}C_{carb}$ values below the climax is only recognized in the Zalidou section and is dated to the *O. nicklesi* StSz. This interval may be missing in the other sections due to a strong erosion expressed by the sedimentary discontinuities (D6–D7 merged; Figs. 4–5, 7).

5. Discussion

The detailed zonations based on ammonite and calcareous nannofossil data allow to date accurately the significant changes in $\delta^{13}C_{carb}$ values and to ascribe an age for the sedimentary discontinuities observed in the EAB. This integrated zonal scheme supports detailed correlations of these events with those recorded in other basins of the northern Tethyan margin, for which integrated stratigraphic studies were also made. In the following parts, comparisons are mainly proposed with SE France and occasionally with other areas.

5.1. Inter-basin correlation of carbon isotopic events

The Weissert Event recorded in the EAB is here compared with carbon isotope data available in SE France, only if constrained by ammonite and nannofossil biostratigraphy (Hennig et al., 1999; Duchamp-Alphonse et al., 2007; McArthur et al., 2007; Gréselle et al., 2011; Kujau et al., 2012; Martinez et al., 2013, 2015; Gollain et al., 2019). For the "*T.*" *pertransiens* StZ and the lower part of the *N. neocomiensiformis* StZ, the carbon isotope data of the Angles section (Valanginian hypostratotype, SE France; Duchamp-Alphonse et al., 2007) were added on the Vergol-La Charce composite section representing the Vocontian Basin succession (Fig. 13). This part of the curve (dashed line) must be interpreted carefully as it is challenging to establish correlations between the Vergol-La Charce and Angles sections. The log of the Angles section given by Duchamp-Alphonse et al. (2007) is not detailed, and the lower Valanginian ammonite zonal scheme was not improved since Busnardo and Thieuloy (1979; see Bulot and Thieuloy, 1995).

A slight decrease in $\delta^{13}C_{carb}$ values (around −0.5‰) is observed from the lower part of "*T.*" *pertransiens* StZ to the lower part of *N. neocomiensiformis* StZ; an increase of a same order is recorded in the upper part of this zone. A similar trend (with a stronger amplitude, around ±1‰) is recorded in some sections of the EAB as Ait Hamouch and Zaouia Sidi Abderahmane (Figs. 4–5). In SE France (Gréselle et al., 2011; Martinez et al., 2015; Gollain et al., 2019; Fig. 13) and SE Spain (Aguado et al., 2018), detailed biostratigraphic data show that the onset of the CIE occurs in the *K. inostranzewi* StZ, more precisely below the boundary between *K. inostranzewi* StSz and *N. platycostatus* StSz (lowest values of $\delta^{13}C$; 0.14‰ and 0.1‰, respectively). In the *K. inostranzewi* StSz, the pre-CIE $\delta^{13}C$ curve shows oscillations between 0.4‰ and 1‰. In the Vocontian Basin, the basal part of this subzone is characterized by four organic-matter-rich layers (Barrande layers; Reboulet et al., 2003) that are not observed in the studied Moroccan area. In some sections of the EAB, low $\delta^{13}C_{carb}$ values are recorded in the *K. inostranzewi* StZ and were interpreted as the onset of the CIE (Aït Hamouch and Zaouia Sidi Abderahmane; Figs. 4–5). At Zalidou, two negative peaks are observed in the *K. inostranzewi* StZ (Figs. 3, 13). The first one (−2.7‰), located at the base, is followed by an increase of isotopic values that continues until the lower part of the *N. peregrinus* StZ. A single point, located at the top of the *K. inostranzewi* StZ, is clearly outside of this curve trend. As it is the lowest value recorded in the Zalidou section (−2.8‰), this might correspond to the onset of the CIE. This would be in agreement with observations made on the Aït Hamouch and Zaouia Sidi Abderahmane sections, for which the CIE starts in the interval between discontinuities D4 and D5 (Figs. 4–5). However, as the onset of the CIE occurs only few metres above the SB F defined by Gréselle and Pittet (2010) in the Vocontian Basin (Fig. 13), the isotopic event may start with D4 (or close to this discontinuity) at Zalidou. As a matter of fact, part of the time recorded by deposits in the deep Vocontian Basin is most probably lacking in the EAB, where D4 corresponds to a major emergence surface, on which sedimentation resumed later than in the Vocontian Basin. This interpretation is consistent with the calcareous nannofossils data at Aït Hamouch and Zalidou, which show that the beginning of the Weissert Event is characterized by the FO of *H. circumradiatus* and by a decrease in the nannoplankton production (Shmeit et al., 2022). Consequently, the onset of the CIE at Zalidou may be placed at the first negative shift in $\delta^{13}C_{carb}$ values (−2.7‰), i.e. at the base of the *K. inostranzewi* StZ (Fig. 3). Diagenetic impacts on platform carbonates during emergence periods and meteoritic diagenesis (Godet et al., 2016) may explain the strong negative values observed just below D5 at Zalidou ($\delta^{13}C_{carb} = -2.8‰$), as well as immediately below D8 at Ait Hamouch ($\delta^{13}C_{carb} = -5.9‰$; Fig. 13).

In the Vocontian Basin, the maximum of $\delta^{13}C_{carb}$ values is recorded in the *S. verrucosum* StZ (double peaks in the *S. verrucosum* StSz; Duchamp-Alphonse et al., 2007; McArthur et al., 2007; Kujau et al., 2012; Martinez et al., 2015; Gollain et al., 2019). This trend in the isotopic curve is not recorded in the EAB. It can be partly explained by condensed intervals and/or stratigraphic gaps around the lower–upper Valanginian boundary; the *S. verrucosum* StZ was partly (Zalidou, Zaouia Sidi Abderahamane) or not (Aït Hamouch; see AH89 and comments on ammonite biostratigraphy) recognized. In these Moroccan sections, the maximal values are observed in the *N. peregrinus* StZ and may correspond to the plateau of high values recorded in the *N. peregrinus* StZ in SE France (Martinez et al., 2015; Fig. 13) and SE Spain (Aguado et al., 2018). In both latter areas, as in the EAB, the carbon isotope curve is characterized by a slow decrease of $\delta^{13}C_{carb}$ values that starts in the uppermost part of the *N. peregrinus* StZ (Ait Hamouch and Zaouia Sidi Abderrahmane), more precisely at the top part of the *O. nicklesi* StSz (Zalidou), and continues in the *C. furcillata* StZ (Zalidou, Ait Hamouch, Zaouia Sidi Abderrahmane, and Ida w Iddar sections; Figs. 3–5, 7). Thus, except for the interval corresponding to the *S. verrucosum* StZ, the main trends of the Valanginian carbon isotope curve in the northern Tethyan basins are similarly observed in the EAB.

5.2. Inter-basin correlation of discontinuities

The EAB is correlated mainly with the SE France Basin, for which biostratigraphic, isotopic and sedimentologic data are all available and a platform-basin transect for the Valanginian depositional system was already established (Arnaud et al., 1981; Reboulet, 1996; Gréselle and Pittet, 2010 and references therein). Thus, the French and Moroccan basins are relevant areas to illustrate the North and South Tethyan margins, respectively.

In the northern Vocontian Basin, Gréselle and Pittet (2010) identified five major sequence boundaries in the Valanginian succession. Their discontinuity "D", at the Berriasian–Valanginian boundary (lowermost part of the "*T.*" *pertransiens* StZ *sensu* Kenjo et al., 2021), corresponds to our SB D1. This discontinuity seems largely identified in SE France, since a basal Valanginian discontinuity (between their "*Thurmanniceras*" *otopeta* (sub-)zone and "*T.*" *pertansiens* ammonite zone) has been identified in the Subalpine

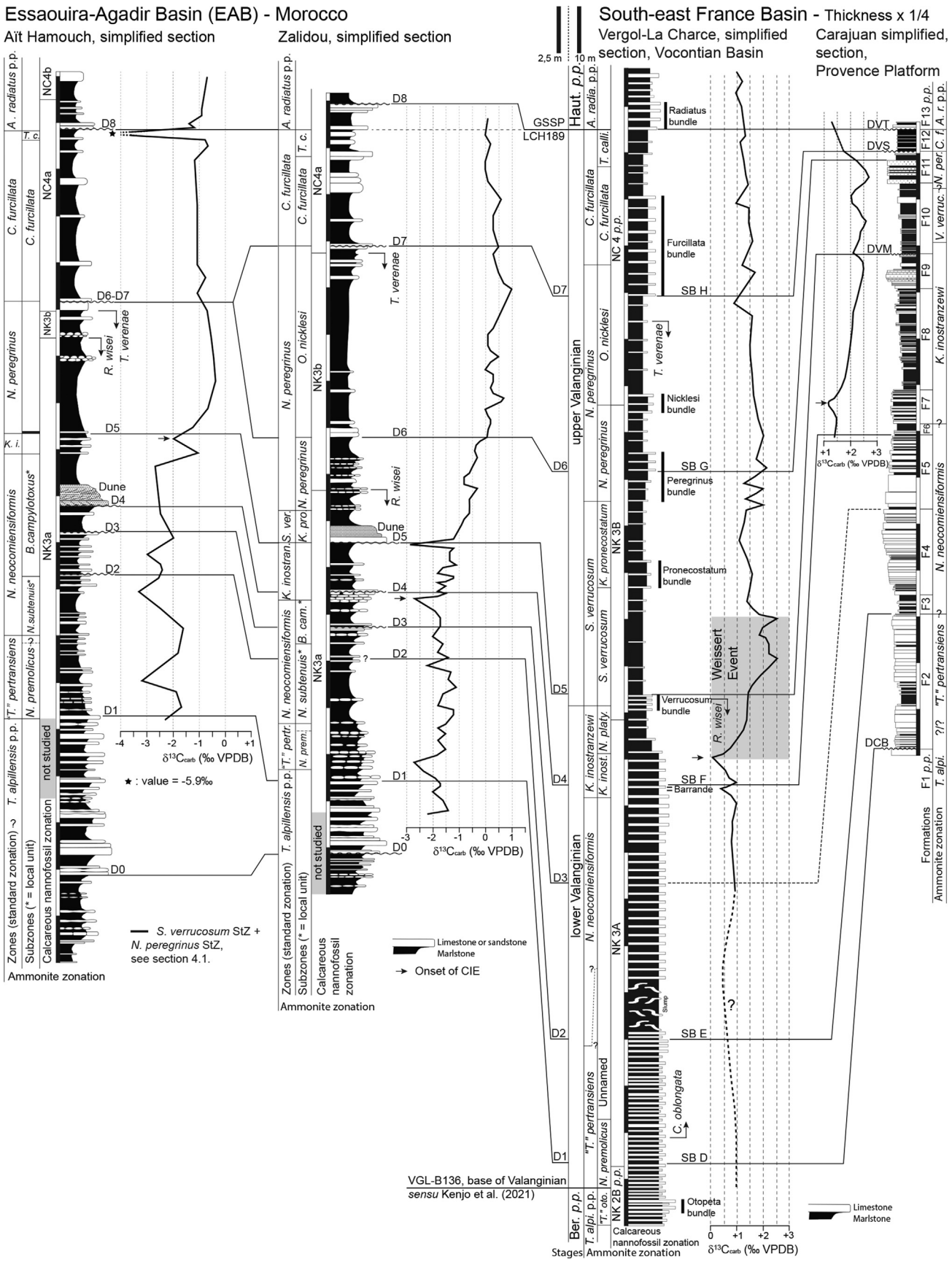

Fig. 13. Correlations of the Essaouira-Agadir Basin (South Tethyan margin) with the south–east France Basin (North Tethyan margin). Lithological successions and carbon isotopic curves are simplified: Zalidou and Aït Hamouch sections after this work (Figs. 3 and 4, respectively); Vergol-La charce composite section (Vocontian Basin) modified after Reboulet

chain by Arnaud et al. (1981; their D-VI) and Morales et al. (2013; their SBe), and in the Provence Platform (DCB of Bulot et al., 1995, 1997). Like in the EAB, these surfaces separate the underlying carbonate shelf from overlying marlstone and limestone, locally sandy. Discontinuity "E" (Gréselle and Pittet, 2010), ascribed to the lower part of the *N. neocomiensiformis* StZ, likely correlates with D-VII of Arnaud et al. (1981), SBf of Morales et al. (2013) and D2 of this work. Discontinuity D3 of the EAB, ascribed to the upper part of the *N. neocomiensiformis* StZ (middle part of the *B. campylotoxus* LSz) may be correlated with the minor discontinuity placed by Gréselle and Pittet (2010, their fig. 14) between their V4 and V5 sequences.

In SE France, the interval around the lower–upper Valanginian boundary is marked by two successive discontinuities: D-VIII and D-IX of Arnaud et al. (1981). According to their correlations with the Angles section (fig. 6 of Arnaud et al., 1981) and according to the standard zonation used here in the Vocontian Basin composite section (Fig. 13), D-VIII and D-IX may correspond to the basal (SB F) and top discontinuities of sequence V6 in Gréselle and Pittet (2010), ascribed to the basal parts of the *K. inostranzewi* StZ and *S. verrucosum* StZ, respectively. According to Bulot (1995, p. 246; see also Bulot et al., 1997), the mid–Valanginian discontinuity of Masse and Lesbros (1987; "discontinuité médiovalanginienne") and the discontinuity of the middle Valanginian (DVM *sensu* Autran, 1993), dated to the basal and top parts of the *K. inostranzewi* zone, respectively, are distinct, contrary to the suggestion of Autran (1993), who correlated them. This discrepancy in interpretations may be due to the very shallow depositional environments at that time, and correlative emergence periods, subsequent erosion and/or amalgamation of discontinuity surfaces (Arnaud et al., 1981; Masse and Lesbros, 1987; Autran, 1993; Bulot, 1995; Bulot et al., 1995, 1997, 2010; Gréselle and Pittet, 2010; Morales et al., 2013), as observed in the Moroccan studied area. In the EAB, as D4 is ascribed to the *K. inostranzewi* StZ in the Zalidou (Fig. 13), Zaouia Sidi Abderahmane and Obbay sections, this discontinuity may be correlated with D-VIII of Arnaud et al. (1981) and with discontinuity "F" of Gréselle and Pittet (2010). In both areas, this discontinuity marks a major facies change, corresponds to the shallowest part of the succession and is unconformable onto previous deposits. D4 may correspond to the "discontinuité médiovalanginienne" of Masse and Lesbros (1987). As observed in the Aït Hamouch and Zaouia Sidi Abderahmane sections (see previous explanations for Zalidou) and in SE France (Vocontian Basin and Provence Platform; Fig. 13), D4 and SB F, respectively, are followed by a negative shift in $\delta^{13}C_{carb}$ values corresponding to the onset of the CIE. Discontinuity D5 caps a depositional sequence that onlaps onto the D4 major discontinuity and thus wedges out eastward (Fig. 12), while D4 is merged with D5 in the Igouzoulen and Ida w Iddar sections of the EAB (Fig. 11). D5 is identified at the lower–upper Valanginian boundary (*K. inostranzewi* StZ–*S. verrucosum* StZ boundary) in the Zalidou, Ida w Iddar and Obbay sections (Figs. 3, 7–8); this discontinuity is ascribed to the basal part of the *S. verrucosum* StZ at Zaouia Sidi Abderahmane and Igouzoulen (Figs. 5–6). Therefore, D5 should be correlated with D-IX of Arnaud et al. (1981), the DVM of Autran (1993) and with the minor SB that separates V6 and V7 sequences of Gréselle and Pittet (2010).

In the EAB, where overlain by the Va6 sequence, D6 occurred in the top part of the *N. peregrinus* StSz at Zalidou and Obbay sections (Figs. 3, 8), where the *O. nicklesi* StSz was recognized. In successions of the Vocontian Basin, Reboulet et al. (1992) mentioned a SB that underlines Lowstand deposits ("Faisceau median" or "Peregrinus bundle", La Charce section) dated to the *N. peregrinus* StSz (Reboulet and Atrops, 1999), while Gréselle and Pittet (2010) identified their discontinuity G also in the lower part of the same (Sub-)zone. Therefore, these events likely correlate with the D6 of the EAB (Fig. 13).

In SE France, Autran (1993) identified a major discontinuity in the upper Valanginian, namely the upper Valanginian discontinuity (DVS), ascribed by this author to the former *H. trinodosum* Zone (equivalent to the *O. nicklesi* StSz and *C. furcillata* StSz). According to biostratigraphic data provided by Reboulet (1996), the DVS occurs at the *N. peregrinus* StZ–*C. furcillata* StZ boundary. Consequently, this discontinuity may be correlated with our D7 since the latter is also situated between these standard zones (Zalidou and Obbay sections). The D7 is responsible for the partial or total erosion of our Va6 depositional sequence and is frequently merged with D6 (Figs. 10–11). Consistently, the DVS is associated in SE France with erosions that may remove down to the middle Valanginian discontinuity *sensu* Autran (1993; DVM). Studying basinal successions, Reboulet et al. (1992) defined a SB discontinuity at the base of thick Lowstand deposits (Furcillata calcareous bundle in Fig. 13) encompassing the upper part of the *O. nicklesi* StSz and the lower part of the *C. furcillata* StSz. Since there are probably no Lowstand deposits in the EAB, the SB of Reboulet et al. (1992) likely correlates with the D7 of the EAB. It also correlates with discontinuity H of Gréselle and Pittet (2010), placed at the top of the *O. nicklesi* StSz. Nevertheless, the latter authors interpret the D5–D7 interval as a period of sea level fall following a major transgression, whereas we interpret the same interval in the EAB as a transgressive–regressive cycle, the maximum flooding of which is placed in the *O. nicklesi* StSz.

In the EAB, D8 is placed at the Valanginian–Hauterivian boundary (Aït Hamouch and Zaouia Sidi Abderahmane; Figs. 4–5) or in the lowermost part of the lower Hauterivian *A. radiatus* StZ (Zalidou, Fig. 3). This discontinuity corresponds to a strong regression. It correlates, in SE France (Fig. 13), with the major surface D-X of Arnaud et al. (1981), with the base of Lowstand deposits of Reboulet et al. (1992), with the top of the V12 sequence of Gréselle and Pittet (2010), and with the uppermost Valanginian discontinuity (DVT of Bulot et al., 2010; see also Reboulet, 1996, p. 275). In SE France, this discontinuity corresponds to a hiatus in shelf areas and may comprise several surfaces (Bulot et al., 2010).

5.3. Sea level changes and sequence origin

The comparisons exposed above show that most of the discontinuities identified in the EAB are also known elsewhere, especially in SE France. This strongly suggests that eustacy controlled the evolution of both areas. Following the two Berriasian sequences, which express a transgressive trend with respect to the base of the sections, the Valanginian succession can be divided into three main transgressive–regressive cycles,

(1996), Gollain et al. (2019) and Kenjo et al. (2021), and completed for the lower Valanginian *p.p* by the isotopic data (dashed line) from the Angles section (Duchamp-Alphonse et al., 2007); Carajuan section (Provence Platform) modified after Bulot (1995), Reboulet (1996), Reboulet et al. (2003) and Gréselle and Pittet (2010). Note that the thickness scale of south–east France sections is 25% that of the Moroccan sections. For the Vocontian basinal section, the calcareous bundles are indicated and named according to the ammonite zonation; "Barrande" correspond to four organic-matter-rich layers (Reboulet et al., 2003); the shaded area is the interval of the Weissert Event from the onset of the carbon isotope excursion (CIE, indicated by a black arrow) until its climax (according to Erba et al., 2004). For the Carajuan section, F1–F13 correspond to some sedimentary formations (see references above); the zonal scheme was updated according to the standard zonation (Reboulet et al., 2018). D1–D8: Moroccan discontinuities after this work (Figs. 3–4); DCB: "Discontinuité au toit des Calcaires Blancs" after Bulot et al. (1995, 1997); SB D to SB H: discontinuities of Gréselle and Pittet (2010); DVM and DVS: "discontinuité du Valanginien moyen" and "discontinuité du Valanginien supérieur" of Autran (1993), respectively; DVT: "discontinuité du Valanginien terminal" of Bulot et al. (2010).

divided by the main discontinuities D4 and D7 (Fig. 12). The first one includes Va1 to Va3, the second one comprises Va4 to Va6, and the third one is made of the Va7 sequence. The maximum flooding of the first cycle occurred during the lower part of the *N. neocomiensiformis* Stz, namely the *N. subtenuis* LSz; the maximum depositional depth of the second cycle seems to be reached in the *O. nicklesi* StSz, and a third maximum flooding is reached during the *C. furcillata* StSz.

The Va2 and Va3 sequences encompass a period of low sea level (Haq, 2014), which culminates with the major D4 discontinuity. The latter is marked by deeply karstified surfaces amalgamating several discontinuities in the proximal northern sections and is overlain by the Va4 sequence that onlaps toward the north or northeast. In the southern part of the EAB, the "mid-−Valanginian events" of Masse and Lesbros (1987) are represented by at least three discontinuities, materialized by erosional surfaces in the southern sections. These discontinuities bound depositional sequences marked by an open marine fauna indicating an outer shelf environment, which suggests that sea level oscillations were of high amplitude. Moreover, in the Aït Hamouch section, the Va2, Va3, and part of the Va4 sequences belong to the *B. campylotoxus* LSz. According to Martinez et al. (2013), the duration of the *B. campylotoxus* subzone is estimated at 390 ky. Since their work, the conception of some zones or sub-zones has changed for the upper part of the lower Valanginian with the introduction of the *N. neocomiensiformis* StZ and *K. inostranzewi* StZ (Reboulet et al., 2014, p. 128−129 and tab. 2). Accordingly, the conception of the *B. campylotoxus* LSz used in the EAB sections would correspond to a larger stratigraphic interval in the Vergol section (Vocontian Basin) than considered in the work of Martinez et al. (2013). Consequently, the duration of the Moroccan *B. campylotoxus* LSz would be higher than 390 ky and may be estimated at around 570 ky. This means that the average duration of the sequences identified in the Aït Hamouch section is around 200 ky. Although not conclusive, these observations are consistent with an orbitally-driven, glacio-eustatic origin for these rapid and high amplitude sea level fluctuations, as suggested for the "middle Valanginian" (Price, 1999; Gréselle and Pitet, 2010; Martinez et al., 2013; Charbonnier et al., 2020).

As a whole, the second and third cycles present deeper depositional environments than the first one, expressing a rise in sea level, likely responsible for the drowning of the lower Valanginian carbonate shelf in the EAB, as well as around the world (Föllmi, 2012). Additionally, the upper Valanginian deposits are more clayey than the lower Valanginian first cycle, suggesting an increase of terrigenous supply. Such change has been observed elsewhere in the world, and interpreted as a change toward more humid conditions (e.g., Schlager, 1980; Bulot et al., 1997; Föllmi, 2012; Bottini et al., 2018).

In SE France, Masse and Lesbros (1987) noted that what they call the "mid−Valanginian events" are associated with a sharp deepening of the depositional environments and with the development of gravitationally reworked sediments, as well as significant terrigenous input (Duchamp-Alphonse et al., 2007). They propose, therefore, that the area was submitted to tectonic movements of the basement (Masse and Lesbros, 1987; Bulot et al., 1997). A partly tectonic origin has also been suggested for the major discontinuity observed around the lower−upper Valanginian boundary in Argentina (Schwarz and Buatois, 2012), and although less accurately dated, in Romania (Gradinaru et al., 2016), and Sardinia (Bottini et al., 2018). In the EAB, neither synsedimentary deformation features nor sharp subsidence changes have been observed around the lower−upper Valanginian boundary. However, as in SE France, the upper Valanginian deposits are marked by a significantly higher amount of terrigenous sediments (sand and silt), especially in the northeastern sections (Fig. 12). This may indicate an erosion resumption in the present-day High Atlas, which may have been triggered by tectonic movements. Nevertheless, since most of the discontinuities identified in the EAB are also known in other areas of the world, these possible tectonic movements were mild enough not to disturb the eustatic signal.

6. Conclusion

The integrated study (ammonites, calcareous nannofossils, sedimentology, sequence stratigraphy, carbon isotopes) of the upper Berriasian−lowermost Hauterivian interval along six sections (Zalidou, Aït Hamouch, Zaouia Sidi Abderahmane, Igouzoulen, Ida w Iddar and Obbay) located in the Essaouira-Agadir Basin (Morocco, South Tethyan margin) led to the following major results.

1. A systematic revision of the whole ammonite fauna was made and the stratigraphic distributions of taxa are given for all studied sections. The analysis of their ranges allowed the establishment of a detailed zonal scheme, more particularly for the lower Valanginian. It corresponds to the standard zonation (Reboulet et al., 2018) for the Mediterranean Province of the Mediterranean−Caucasian Subrealm (Tethyan Realm). Two local subzones were added in the *Neocomites neocomiensiformis* Standard Zone, which is recognized for the first time in the Moroccan lower Valanginian successions. The base of the Valanginian and that of the upper Valanginian are placed at the base of the "*Thurmanniceras*" *pertransiens* Standard Zone and that of *Saynoceras verrucosum* Standard Zone, respectively.
2. A calcareous nannofossil biostratigraphy was established in the most suitable sections (Zalidou and Aït Hamouch) for nannofossil studies (Shmeit et al., 2022; this work). The calcareous nannofossil zonal schemes of Sissingh (1977) and Bralower et al. (1995) are recognized, and a sequence of seven nannofossil bioevents is identified. Thus, ammonite and nannofossil zonations are calibrated for these reference sections.
3. Detailed sedimentological field and microfacies analysis, led to recognize sedimentary discontinuities (D0 to D8), which allowed a sequence stratigraphic analysis of the basin. Two depositional sequences are recognized in the Berriasian (Be1 and Be2), seven in the Valanginian (Va1 to Va7) and one in the Hauterivian (Ha1). Major discontinuities resulted in significant erosions that led locally to amalgamated surfaces, at the lower−upper Valanginian boundary interval (D4−D5) and in the middle part of the upper Valanginian (D6−D7).
4. Carbon isotope analyses were made in five sections. The Weissert Event is well recorded in the highest resolution $\delta^{13}C_{carb}$ curve obtained in this study (Zalidou). The mid−Valanginian carbon isotope excursion is also relatively well observed at Aït Hamouch and Zaouia Sidi Abderahmane, but more cautiously interpreted elsewhere. The precise age of its onset is obscured by the major "mid−Valanginian" eustatic regression that led to a widespread emergence, erosions, and sedimentary hiatuses (D4−D5).
5. The Valanginian carbon isotope record observed in the Essaouira-Agadir Basin is similar to those recorded in the south−east France Basin. The Moroccan sedimentary discontinuities can be correlated with those identified in south−east France, suggesting that eustacy mainly controlled the evolution of both depositional areas.

Data availability

Isotopic and calcareous nannofossil data are available in Supplementary Material.

Acknowledgements

Our project on the Essaouira-Agadir Basin benefited of financial supports from a project (2013–2015) funded by the Moroccan and French Ministries of foreign affairs (Partenariat Hubert Curien, Volubilis n° 031/STU/13), from the French IRD, Campus France, and various grants from ISTerre, the Laboratoire de Géologie de Lyon, the OSUG@2020 Labex, the CNRS SYSTER program and IODP France soutien post-cruise. Christophe Despierres (Grenoble) and Thomas Letulle (Lyon) are thanked for their contribution to this study through Master memoirs. We acknowledge Emmanuel Robert (University of Lyon) for help in completing the macrofossil sampling in some sections. We are indebted to Mohssine Ettachfini (University of Marrakech, Morocco), who gave full access to his ammonite collections and made helpful suggestions. We are extremely grateful to Miguel Company (University of Granada, Spain) for fruitful discussions on ammonites. We are grateful to the editor Eduardo Koutsoukos, Beatriz Aguirre-Urreta and an anonymous reviewer for both corrections and comments which greatly improved the quality of an earlier version of the manuscript.

References

Aguado, R., Company, M., Tavera, J.M., 2000. The Berriasian/Valanginian boundary in the Mediterranean region: new data from the Caravaca and Cehegín sections, SE Spain. Cretaceous Research 21, 1–21.

Aguado, R., Company, M., Castro, J.M., de Gea, G.A., Molina, J.M., Nieto, L.M., Ruiz-Ortiz, P.A., 2018. A new record of the Weissert episode from the Valanginian succession of Cehegín (Subbetic, SE Spain): bio- and carbon isotope stratigraphy. Cretaceous Research 92, 122–137.

Aguirre-Urreta, M.B., Alvarez, P.P., 1999. The Berriasian genus *Groebericeras* in Argentina and the problem of its age. Scripta Geologica Special Issue 3, 15–29.

Aguirre-Urreta, B., Martinez, M., Schmitz, M., Lescano, M., Omarini, J., Tunik, M., Kuhnert, H., Concheyro, A., Rawson, P.F., Ramos, V.A., Reboulet, S., Noclin, N., Frederichs, T., Nickl, A.-L., Pälike, H., 2019. Interhemispheric radio-astrochronological calibration of the time scales from the Andean and the Tethyan areas in the Valanginian–Hauterivian (Early Cretaceous). Gondwana Research 70, 104–132.

Algouti, A., Algouti, A., Taj-Eddine, K., 1999. Le Sénonien du Haut Atlas occidental, Maroc: sédimentologie, analyse séquentielle et paléogéographie. Journal of African Earth Sciences 29, 643–658.

Ambroggi, R., 1963. Etude géologique du versant méridional du Haut Atlas occidental et de la plaine du Souss. Notes du Service Géologique du Maroc 157, 1–321.

Applegate, J.L., Bergen, J.A., 1988. Cretaceous calcareous nannofossiil biostratigraphy of sediments recovered from the Galicia margin, ODP Leg 103. Proc. In: Boillot, G., Winterer, E.L., et al. (Eds.), Proceedings of the Ocean Drilling Program, Scientific Results, vol. 103. (Ocean Drilling Program), College Station, TX, pp. 293–348.

Arnaud, H., Gidon, M., Thieuloy, J.-P., 1981. Les Calcaires du Fontanil des environs de Grenoble: leur place dans la stratigraphie du Néocomien entre le Jura et le domaine vocontien. Eclogae Geologicae Helvetiae 74, 109–137.

Autran, G., 1993. L'évolution de la marge nord-est provençale (Arc de Castellane) du Valanginien moyen à l'Hauterivien à travers l'analyse biostratigraphique des séries de la région de Peyroules: séries condensées, discontinuités et indices d'une tectogenèse distensive. Paléobiologie. Annales du Muséum d'Histoire Naturelle de Nice 10, 1–240.

Ben Ammar, S., Layeb, M., 2021. Updated geochemical insights on the Weissert and Faraoni events in the southern Tethyan margin (northern Tunisia). Arabian Journal of Geosciences 14, 2379.

Bergen, J.A., 1994. Berriasian to early Aptian calcareous nannofossils from the Vocontian trough (SE France and deep sea drilling site 534: new nannofossil taxa and a summary of low-latitude biostratigraphic events. Journal of Nannoplankton Research 16, 59–69.

Blanc, E., Bulot, L.G., Paicheler, J.C., 1994. La coupe de référence de Montbrun-les-Bains (Drôme, SE France): un stratotype potentiel pour la limite Berriasien–Valanginien. Comptes Rendus de l'Académie des Sciences de Paris 318 (sér. II), 101–108.

Bottini, C., Dieni, I., Erba, E., Massari, F., Weissert, H., 2018. The Valanginian Weissert oceanic anoxic event recorded in central-eastern Sardinia (Italy). Rivista Italiana di Paleontologia e Stratigrafia 124 (3), 617–637.

Bouatmani, R., Chakor Alimi, A., Medina, F., 2007. Subsidence, évolution thermique et maturation des hydrocarbures dans le bassin d'Essaouira (Maroc): apport de la modélisation. Bulletin de l'Institut Scientifique Rabat 29, 15–36.

Bourgeoini, Y., Ali Nabiha, B.H., Saloua, R., Kamal, T., 2002. Etude biostratigraphique du Crétacé inférieur (Barrémien supérieur-Albien) du Haut Atlas Occidental (Maroc). Estudios Geológicos 58, 109–116.

Bown, P.R., Concheyro, A., 2004. Lower Cretaceous calcareous nannoplankton from the Neuquén Basin, Argentina. Marine Micropaleontology 52, 51–84.

Bralower, T.J., 1987. Valanginian to Aptian calcareous nannofossil stratigraphy and correlation with the upper M-sequence magnetic anomalies. Marine Micropaleontology 11, 293–310.

Bralower, T.J., Monechi, S., Thierstein, H.R., 1989. Calcareous nannofossil zonation of the Jurassic-Cretaceous boundary interval and correlation with the geomagnetic polarity timescale. Marine Micropaleontology 14, 153–235.

Bralower, T.J., Leckie, R.M., Sliter, W.V., Thierstein, H.R., 1995. An Integrated Cretaceous Microfossil Biostratigraphy. Geochronology Time Scales and Global Stratigraphic Correlation, vol. 54. Society of Economic Paleontologists and Mineralogists Special Publication, pp. 65–79.

Bralower, T.J., Premoli Silva, I., Malone, M.J., 2002. Shipboard scientific party, 2002. Site 1213. In: Bralower, T.J., Premoli Silva, I., Malone, M.J., et al. (Eds.), Proceedings of the Ocean Drilling Project, Initial Reports 198, pp. 1–110.

Bulot, L.G., 1995. Les formations à ammonites du Crétacé inférieur dans le Sud-Est de la France (Berriasien à Hauterivien): biostratigraphie, paléontologie et cycles sédimentaires. Unpublished PhD thesis. Muséum National d'Histoire Naturelle, Paris, p. 398.

Bulot, L.G., Thieuloy, J.-P., 1995. Les biohorizons du Valanginien du Sud-Est de la France: un outil fondamental pour les corrélations au sein de la Téthys occidentale. Géologie Alpine, Mémoire Hors Série 20 (1994), 15–41.

Bulot, L.G., Thieuloy, J.-P., Blanc, E., Klein, J., 1993. Le cadre stratigraphique du Valanginien supérieur et de l'Hauterivien du Sud-Est de la France: définition de biochronozones et caractérisation de nouveaux biohorizons. Géologie Alpine 68, 13–56.

Bulot, L.G., Thieuloy, J.-P., Arnaud, H., Delanoy, G., 1995. The Lower Cretaceous Cephalopod team first field meeting (Digne, 1990). The Lower Cretaceous of the South Vocontian basin and margins. In: Bulot, et al. (Eds.), Lower Cretaceous cephalopod biostratigraphy of the Western Tethys: recent developments, regional synthesis and outstanding problems, Géologie Alpine (1994), H.S., vol. 20, pp. 383–399.

Bulot, L.G., Masse, J.-P., Moutier, L., Virgonne, A., 1997. Organisation stratigraphique et dynamique sédimentaire du Valanginien au passage plate-forme/bassin en Basse-Provence (S-E France). Bulletin de la Société Géologique de France 168, 171–179.

Bulot, L.G., Vermeulen, J., Grosheny, D., 2010. Le Crétacé de l'Arc de Castellane (SE France, 25-28 Août 2010). Excursion du Groupe Français du Crétacé, GFC 2010. Série « Excursion », p. 46. https://hal.archives-ouvertes.fr/hal-00686778.

Busnardo, R., Thieuloy, J.P., 1979. Les zones d'ammonites du Valanginien. In: Busnardo, R., Thieuloy, J.P., Moullade, M. (Eds.), Hypostratotype mésogéen de l'étage Valanginien (sud-est de la France). Edition C.N.R.S (Paris), Les stratotypes français, vol. 6, pp. 58–68.

Busnardo, R., Charollais, J., Weidmann, M., Clavel, B., 2003. Le Crétacé inférieur de la Veveyse de Châtel (Ultrahelvétique des Préalpes externes ; canton de Fribourg, Suisse). Revue de Paléobiologie 22, 1–174.

Canérot, J., Cugny, P., Peybernès, B., Rahli, I., Rey, J., Thieuloy, J.-P., 1986. Comparative study of the Lower and Mid-Cretaceous sequences on different maghrebian shelves and basins: Their place in the evolution of the North African, Atlantic and Neotethysian margins. Palaeogeography, Palaeoclimatology, Palaeoecology 55, 213–232.

Charbonnier, G., Morales, C., Duchamp-Alphonse, S., Westermann, S., Adatte, T., Follmi, K.B., 2017. Mercury enrichments indicate volcanic triggering of Valanginian environmental change. Scientific Reports 7, 40808.

Charbonnier, G., Duchamp-Alphonse, S., Deconinck, J.-F., Adatte, T., Spangenberg, J.E., Colin, C., Follmi, K.B., 2020. A global palaeoclimatic reconstruction for the Valanginian based on clay mineralogical and geochemical data. Earth-Science Reviews 202, 103092.

Coffin, M.F., Eldholm, O., 1994. Large igneous provinces: crustal structure, dimensions, and external consequences. Reviews of Geophysics 32, 1–36.

Company, M., 1987. Los ammonites del Valanginiense del sector oriental de las Cordilleras Béticas (SE de España). Tesis Doctoral, Universidad de Granada, Granada, p. 294.

Company, M., Tavera, J.M., 2015. Lower Valanginian ammonite biostratigraphy in the Subbetic Domain (Betic Cordillera, southeastern Spain). Carnets de Géologie 15, 71–88.

Duchamp-Alphonse, S., Gardin, S., Fiet, N., Bartolini, A., Blamart, D., Pagel, M., 2007. Fertilization of the northwestern Tethys (Vocontian basin, SE France) during the Valanginian carbon isotope perturbation: Evidence from calcareous nannofossils and trace element data. Palaeogeography, Palaeoclimatology, Palaeoecology 243, 132–151.

Duffaud, F., Brun, L., Plauchut, B., 1966. Le bassin du Sud-Ouest Marocain. In: Reyre, D. (Ed.), Bassins sédimentaires du littoral Africain. Association des Services Géologiques Africains. Firmin Didot Publ, Paris, pp. 5–12.

Ellouz, N., Patriat, M., Gaulier, J.-M., Bouatmani, R., Sabounji, S., 2003. From rifting to Alpine inversion: Mesozoic and Cenozoic subsidence history of some Moroccan basins. Sedimentary Geology 156, 185–212.

Erba, E., Bartolini, A., Larson, R.L., 2004. Valanginian Weissert oceanic anoxic event. Geology 32, 149–152.

Ettachfini, M., 1991. Le Valanginien de l'Atlas Atlantique (Maroc): stratigraphie et ammonitofaune. Strata 15 (2), 1–177.

Ettachfini, M., 2004. Les ammonites néocomiennes dans l'Atlas Atlantique (Maroc): biostratigraphie, paléontologie, paléobiogéographie et paléoécologie. Strata 43 (2), 1–225.

Fanti, F., Contessi, M., Franchi, F., 2012. The "Continental Intercalaire" of southern Tunisia: Stratigraphy, paleontology, and paleoecology. Journal of African Earth Sciences 73–74, 1–23.
Ferry, S., Masrour, M., Grosheny, D., 2007. Le Crétacé de la marge atlantique marocaine (région d'Agadir). In: Excursion du Groupe Français du Crétacé, Livret-guide, p. 70. https://hal.archives-ouvertes.fr/hal-00686791/fr/.
Föllmi, K., 2012. Early Cretaceous life, climate and anoxia. Cretaceous Research 35, 230–357.
Föllmi, K.B., Weissert, H., Bisping, M., Funk, H., 1994. Phosphogenesis, carbon–isotope stratigraphy, and carbonate–platform evolution along the Lower Cretaceous northern Tethyan margin. The Geological Society of America Bulletin 106, 729–746.
Frizon de Lamotte, D., Saint Bezar, B., Bracène, R., 2000. The two main steps of the Atlas building and geodynamics of the western Mediterranean. Tectonics 19, 740–761.
Frizon de Lamotte, D., Leturmy, P., Missenard, Y., Khomsi, S., Ruiz, G., Saddiqi, O., Guillocheau, F., Michard, A., 2009. Mesozoic and Cenozoic vertical movements in the Atlas system (Algeria, Morocco, Tunisia): An overview. Tectonophysics 475, 9–28.
Gale, A.S., 2020. Roveacrinidae (Crinoidea, Articulata) from the Cenomanian and Turonian of North Africa (Agadir Basin and Anti-Atlas, Morocco, and central Tunisia): biostratigraphy and taxonomy. Acta Geologica Polonica 70, 273–310.
Gale, A.S., Mutterlose, J., Batenburg, S., with contributions by, Gradstein, F.M., Agterberg, F.P., Ogg, J.G., Petrizzo, M.R., 2020. The Cretaceous Period. In: Gradstein, et al. (Eds.), Geologic Time Scale 2020. Elsevier BV, pp. 1023–1086.
Gauthier, H., Busnardo, R., Combémorel, R., Delanoy, G., Fischer, J.-C., Guérin-Franiatte, S., Joly, B., Kennedy, W.J., Sornay, J., Tintant, H. (Eds.), 2006. Révision critique de la Paléontologie française d'Alcide d'Orbigny (edited by Fischer, J.C.). Volume IV. Céphalopodes crétacés. Backhuys Publisher, Leiden, p. 292.
Godet, A., Durlet, C., Spangenberg, J.E., Föllmi, K.B., 2016. Estimating the impact of early diagenesis on isotope records in shallow-marine carbonates: A case study from the Urgonian Platform in western Swiss Jura. Palaeogeography, Palaeoclimatology, Palaeoecology 454, 125–138.
Gollain, B., Mattioli, E., Kenjo, S., Bartolini, A., Reboulet, S., 2019. Size-patterns of the coccolith *Watznaueria barnesiae* in the Lower Creataceous: biotic *versus* abiotic forcing. Marine Micropaleontology 152, 101740.
Gomes, A.S., Vasconcelos, P.M., 2021. Geochronology of the Paraná-Etendeka large igneous province. Earth-Science Reviews 220, 103716.
Gradinaru, M., Lazar, J., Bucur, I.I., Gradinaru, E., Sasaran, E., Ducea, M.N., Andrasanu, A., 2016. The Valanginian history of the eastern part of the Getic Carbonate Platform (Southern Carpathians, Romania): Evidence for emergence and drowning of the platform. Cretaceous Research 66, 11–42.
Gréselle, B., Pittet, B., 2010. Sea-level reconstructions from the Peri-Vocontian Zone (South-east France) point to Valanginian glacio-eustasy. Sedimentology 57, 1640–1684.
Gréselle, B., Pittet, B., Mattioli, E., Joachimski, M., Barbarin, N., Riquier, L., Reboulet, S., Pucéat, E., 2011. The Valanginian isotope event: A complex suite of palaeoenvironmental perturbations. Palaeogeography, Palaeoclimatology, Palaeoecology 306, 41–57.
Gröcke, D.R., Price, G.D., Robinson, S.A., Baraboshkin, E.Y., Mutterlose, J., Ruffell, A.H., 2005. The Upper Valanginian (Early Cretaceous) positive carbon-isotope event recorded in terrestrial plants. Earth and Planetary Science Letters 240, 495–509.
Guiraud, R., Bosworth, W., 1997. Senonian inversion and rejuvenation of rifting in Africa and Arabia: synthesis and implications to plate-scale tectonics. Tectonophysics 282, 39–82.
Hafid, M., Tari, G., Bouhadioui, D., El Moussaid, I., Aït Salem, A., Nahim, M., Dakki, M., 2008. Atlantic Basins. In: Michard, A., et al. (Eds.), Continental Evolution: the Geology of Morocco. Lecture Notes in Earth Sciences, vol. 116, pp. 303–329.
Haq, B.U., 2014. Cretaceous eustasy revisited. Global and Planetary Change 113, 44–58.
Hedberg, H.D., 1976. International stratigraphic guide. A Guide to Stratigraphic Classification, Terminology, and Procedure. Wiley J. and Sons, New York, p. 200.
Hennig, S., Weissert, H., Bulot, L., 1999. C-isotope stratigraphy, a calibration tool between ammonite- and magnetostratigraphy: the Valanginian–Hauterivian transition. Geologica Carpathica 50, 91–96.
Hoedemaeker, P.J., Reboulet, S., (reporters), Aguirre-Urreta, M.B., Alsen, P., Aoutem, M., Atrops, F., Barragán, R., Company, M., González-Arreola, C., Klein, J., Lukeneder, A., Ploch, I., Raisossadat, N., Rawson, P.F., Ropolo, P., Vašíček, Z., Vermeulen, J., Wippich, M.G.E., 2003. Report on the 1st international workshop of the IUGS Lower Cretaceous Ammonite Working Group, the "Kilian Group" (Lyon, 11 July 2002). Cretaceous Research 24, 89–94 and erratum (p. 805).
Jaillard, E., Al Yacoubi, L., Reboulet, S., Robert, E., Masrour, M., Bouchaou, L., Giraud, F., El Hariri, K., 2019a. Late Barremian eustacy and tectonism in the western High Atlas (Essaouira-Agadir Basin), Morocco. Cretaceous Research 93, 225–244.
Jaillard, E., Hassanein Kassab, W., Giraud, F., Robert, E., Masrour, M., El Hariri, K., Mohamed, F., Aly, M.F., 2019b. Aptian-lower Albian sedimentation in the Essouira-Agadir basin, western Morocco. Cretaceous Research 102, 59–80.
Joly, B., 2000. Les Juraphyllitidae, Phylloceratidae, Neophylloceratidae (Phylloceratoceae, Phylloceratina, Ammonoidea) de France au Jurassique et au Crétacé. Geobios, Mémoire Spécial 23, 1–204.
Kender, S., Kaminski, M.A., 2017. Modern deep-water agglutinated foraminifera from IODP Expedition 323, Bering Sea: ecological and taxonomic implications. Journal of Micropalaeontology 36, 195–218.
Kenjo, S., 2014. Biostratigraphie intégrée à nannofossiles calcaires et ammonoïdes: développement et implications pour la définition et la valorisation des stratotypes d'unité et de limite. L'exemple des étages Berriasien et Valanginien et de leur limite (140 Millions d'années). Unpublished PhD thesis, Université de Lyon, p. 226.
Kenjo, S., Reboulet, S., Mattioli, E., Ma'louleh, K., 2021. The Berriasian–Valanginian boundary in the Mediterranean Province of the Tethyan Realm: Ammonite and calcareous nannofossil biostratigraphy of the Vergol section (Montbrun-les-Bains, SE France), candidate for the Valanginian GSSP. Cretaceous Research 121, 104738.
Kessels, K., Mutterlose, J., Michalzik, D., 2006. Early Cretaceous (Valanginian - Hauterivian) calcareous nannofossils and isotopes of the northern hemisphere: Proxies for the understanding of Cretaceous climate. Lethaia 39, 157–172.
Klein, J., 2005. Lower Cretaceous Ammonites I, Perisphinctaceae 1: Himalayitidae, Olcostephanidae, Holcodiscidae, Neocomitidae, Oosterellidae. In: Riegraf, W. (Ed.), Fossilium Catalogus I: Animalia, Pars 139. Backhuys Publishers, Leiden, Netherlands, p. 484.
Klein, J., Busnardo, R., Company, M., Delanoy, G., Kakabadze, M., Reboulet, S., Ropolo, P., Vašíček, Z., Vermeulen, J., 2007. Lower Cretaceous Ammonites III. Bochianitoidea, Protancyloceratoidea, Ancyloceratoidea, Ptychoceratoidea. In: Riegraf, W. (Ed.), Fossilium Catalogus I: Animalia, Pars 144. Backhuys Publishers, Leiden, Netherlands, p. 381.
Klein, J., Hoffmann, R., Joly, B., Shigeta, Y., Vašíček, Z., 2009. Lower Cretaceous Ammonites IV. Boreophylloceratoidea, Phylloceratoidea, Lytoceratoidea, Tetragonitoidea, Haploceratoidea including the Upper Cretaceous representatives. In: Riegraf, W. (Ed.), Fossilium Catalogus I: Animalia, Pars 146. Backhuys Publishers, Leiden, Netherlands, p. 416.
Kuhnt, W., Moullade, M., Kaminski, M.A., 1996. Ecological structuring and evolution of deep-sea agglutinated foraminifera – A review. Revue de Micropaléontologie 39, 271–281.
Kujau, A., Heimhofer, U., Ostertag-Henning, C., Gréselle, B., Mutterlose, J., 2012. No evidence for anoxia during the Valanginian carbon isotope event – An organic-geochemical study from the Vocontian Basin, SE France. Global and Planetary Change 92–93, 92–104.
Lefranc, J.-P., Guiraud, R., 1990. Continental Intercalaire of northwestern Sahara and its equivalents in the neighbouring regions. Journal of African Earth Sciences 10, 27–77.
Le Hégarat, G., 1973. Le Berriasien du Sud-Est de la France. Documents des Laboratoires de Géologie. Faculté des Sciences de Lyon 43 (1971), 1–576.
Le Roy, P., Guillocheau, F., Piqué, A., Morabet, A.M., 1998. Subsidence of the Atlantic Moroccan margin during the Mesozoic. Canadian Journal of Earth Sciences 35, 476–493.
Lini, A., Weissert, H., Erba, E., 1992. The Valanginian carbon isotope event: a first episode of greenhouse climate conditions during the Cretaceous. Terra Nova 4, 374–384.
Luber, T.L., Bulot, L.G., Redfern, J., Frau, C., Arantegui, A., Masrour, M., 2017. A revised ammonoid biostratigraphy for the Aptian of NW Africa: Essaouira-Agadir Basin. Cretaceous Research 79, 12–34.
Martinez, M., Deconinck, J.-F., Pellenard, P., Reboulet, S., Riquier, L., 2013. Astrochronology of the Valanginian stage from reference sections (Vocontian Basin, France) and palaeoenvironmental implications for the Weissert Event. Palaeogeography, Palaeoclimatology, Palaeoecology 376, 91–102.
Martinez, M., Deconinck, J.-F., Pellenard, P., Riquier, L., Company, M., Reboulet, S., Moiroud, M., 2015. Astrochronology of the Valanginian–Hauterivian stages (Early Cretaceous): chronological relationships between the Paraná–Etendeka large igneous province and the Weissert and the Faraoni events. Global and Planetary Change 131, 158–173.
Masse, J.-P., Lesbros, R., 1987. Evénements géodynamiques médio-valanginiens dans le S-E de la France et leur retentissements bathymétriques. Leur signification dans le cadre géodynamique de la Méditerranée occidentale. Mémoire géologique de l'université de Dijon 11, 149–156.
McArthur, J.M., Janssen, N.M.M., Reboulet, S., Leng, M.J., Thirlwall, M.F., van de Schootbrugge, B., 2007. Palaeotemperatures, polar ice-volume, and isotope stratigraphy (Mg/Ca, $\delta^{18}O$, $\delta^{13}C$, $^{87}Sr/^{86}Sr$): The Early Cretaceous (Berriasian, Valanginian, Hauterivian). Palaeogeography, Palaeoclimatology, Palaeoecology 248, 391–430.
Melinte, M., Mutterlose, J., 2001. A Valanginian (Early Cretaceous) "boreal nannoplankton excursion" in sections from Romania. Marine Micropaleontology 43, 1–25.
Melliti, S., Reboulet, S., Ben Haj Ali, N., Arfaoui, M.S., Zargouni, F., Memmi, L., 2019. Ammonoid and foraminiferal biostratigraphy from uppermost Valanginian to lowermost Barremian of the Jebel Boulahouajeb section (northern Tunisia). Journal of African Earth Sciences 151, 438–460.
Möller, C., Mutterlose, J., Alsen, P., 2015. Integrated stratigraphy of Lower Cretaceous sediments (Ryazanian–Hauterivian) from North-East Greenland. Palaeogeography, Palaeoclimatology, Palaeoecology 437, 85–97.
Morales, C., Gardin, S., Schnyder, J., Spangenberg, J., Arnaud-Vanneau, A., Arnaud, H., Adatte, T., Föllmi, K.B., 2013. Berriasian and early Valanginian environmental change along a transect from the Jura Platform to the Vocontian Basin. Sedimentology 60, 36–63.

Mourgues, F.A., Bulot, L.G., Frau, C., 2015. The Valanginian Olcostephaninae Haug, 1910 (Ammonoidea) from the Andean Lower Cretaceous Chañarcillo Basin, Northern Chile. Andean Geology 42, 213–236.
Mutterlose, J., Rawson, P.F., Reboulet (reporters), S., Baudin, F., Bulot, L., Emmanuel, L., Gardin, S., Martinez, M., Renard, M., 2020. The Global Boundary Stratotype Section and Point (GSSP) for the base of the Hauterivian Stage (Lower Cretaceous), La Charce, southeast France. Episodes, Communication of IUGS Geological Standards 1–22.
Newell, A.J., Kirby, G.A., Sorensen, J.P.R., Milodowski, A.E., 2015. The Cretaceous Continental Intercalaire in central Algeria: subsurface evidence for a fluvial to aeolian transition and implications for the onset of aridity on the Saharan Platform. Palaeogeography, Palaeoclimatology, Palaeoecology 438, 146–159.
Perch-Nielsen, K., 1979. Calcareous nannofossils from the Cretaceous between the North Sea and the Mediterranean. Aspekte der Kreide Europas. IUGS Series A 6, 223–272.
Perch-Nielsen, K., 1985. Mesozoic Calcareous nannofossils. In: Bolli, H.M., Saunders, J.B., Perch-Nielsen, K. (Eds.), Plankton stratigraphy. Cambridge University Press, Cambridge, pp. 329–426.
Price, G.D., 1999. The evidence and implications of polar ice during the Mesozoic. Earth-Science Reviews 48, 183–210.
Pucéat, E., Lecuyer, C., Sheppard, S.M.F., Dromart, G., Reboulet, S., Grandjean, P., 2003. Thermal evolution of Cretaceous Tethyan marine waters inferred from oxygen isotope composition of fish tooth enamels. Paleoceanography 18 (2), 1029.
Rawson, P.F., 2007. Global relationships of Argentine (Neuquén Basin) Early Cretaceous ammonite faunas. Geological Journal 42, 175–183.
Reboulet, S., 1996. L'évolution des ammonites du Valanginien-Hauterivien inférieur du bassin vocontien et de la plate-forme provençale (S-E de la France): relations avec la stratigraphie séquentielle et implications biostratigraphiques. Documents des Laboratoires de Géologie, Lyon 137 (1995), 1–371.
Reboulet, S., 2008. Origination of *Himantoceras* (heteromorphic ammonoids) related to palaeoceanography and climatic changes during the Valanginian. 1st International Meeting on Correlation of Cretaceous Micro- and Macrofossils, Vienna (Austria), 16–18 April, 2008. Berichte der Geologischen Bundesanstalt 74, 89–91.
Reboulet, S., Atrops, F., 1999. Comments and proposals about the Valanginian–lower Hauterivian ammonite zonation of south-eastern France. Eclogae Geologicae Helvetiae 92, 183–197.
Reboulet, S., Atrops, F., Ferry, S., Schaaf, A., 1992. Renouvellement des ammonites en fosse vocontienne à la limite Valanginien–Hauterivien. Geobios 25, 469–476.
Reboulet, S., Mattioli, E., Pittet, B., Baudin, F., Olivero, D., Proux, O., 2003. Ammonoid and nannoplankton abundance in Valanginian (early Cretaceous) limestone-marl successions from the southeast France Basin: carbonate dilution or productivity? Palaeogeography, Palaeoclimatology, Palaeoecology 201, 113–139.
Reboulet, S., Hoedemaeker, P.J., (reporters), Aguirre-Urreta, M.B., Alsen, P., Atrops, F., Baraboshkin, E.Y., Company, M., Delanoy, G., Dutour, Y., Klein, J., Latil, J.L., Lukeneder, A., Mitta, V., Mourgues, F.A., Ploch, I., Raisossadat, N., Ropolo, P., Sandoval, J., Tavera, J.M., Vašíček, Z., Vermeulen, J., 2006. Report on the 2nd international meeting of the IUGS Lower Cretaceous Ammonite Working Group, the "Kilian Group" (Neuchâtel, Switzerland, 8 September 2005). Cretaceous Research 27, 712–715.
Reboulet, S., Klein, J., (reporters), Barragán, R., Company, M., González-Arreola, C., Lukeneder, A., Raisossadat, S.N., Sandoval, J., Szives, O., Tavera, J.M., Vašíček, Z., Vermeulen, J., 2009. Report on the 3rd international meeting of the IUGS Lower Cretaceous Ammonite Working Group, the "Kilian Group" (Vienna, Austria, 15th April 2008). Cretaceous Research 30, 496–502.
Reboulet, S., Rawson, P.F., Moreno-Bedmar, J.A., (reporters), Aguirre-Urreta, M.B., Barragán, R., Bogomolov, Y., Company, M., González-Arreola, C., Idakieva Stoyanova, V., Lukeneder, A., Matrion, B., Mitta, V., Randrianaly, H., Vašíček, Z., Baraboshkin, E.J., Bert, D., Bersac, S., Bogdanova, T.N., Bulot, L.G., Latil, J.-L., Mikhailova, I.A., Ropolo, P., Szives, O., 2011. Report on the 4th international meeting of the IUGS Lower Cretaceous Ammonite Working Group, the "Kilian Group" (Dijon, France, 30th August 2010). Cretaceous Research 32, 786–793.
Reboulet, S., Szives, O., (reporters), Aguirre-Urreta, B., Barragán, R., Company, M., Idakieva, V., Ivanov, M., Kakabadze, M.V., Moreno-Bedmar, J.A., Sandoval, J., Baraboshkin, E.J., Çağlar, M.K., Főzy, I., González-Arreola, C., Kenjo, S., Lukeneder, A., Raisossadat, S.N., Rawson, P.F., Tavera, J.M., 2014. Report of the 5th international meeting of the IUGS Lower Cretaceous Ammonite Working Group, the Kilian Group (Ankara, Turkey, 31st August 2013). Cretaceous Research 50, 126–137.
Reboulet, S., Szives, O., (reporters), Aguirre-Urreta, B., Barragán, R., Company, M., Frau, C., Kakabadze, M.V., Klein, J., Moreno-Bedmar, J.A., Lukeneder, A., Pictet, P., Ploch, I., Raisossadat, S.N., Vašíček, Z., Baraboshkin, E.J., Mitta, V.V., 2018. Report on the 6th International Meeting of the IUGS Lower Cretaceous Ammonite Working Group, the Kilian Group (Vienna, Austria, 20th August 2017). Cretaceous Research 91, 100–110.
Rey, J., Canérot, J., Peybernès, B., Taj-Eddine, K., Rahhali, I., Thieuloy, J.-P., 1986. Le Crétacé inférieur de la région d'Essaouira: données biostratigraphiques et évolutions sédimentaires. In: PICG – UNESCO Section Sciences de la Terre 183, Revue de la Faculté des sciences de Marrakech, Numéro Spécial 2, pp. 413–441.
Rey, J., Canérot, J., Peybernès, B., Taj-Eddine, K., Thieuloy, J.-P., 1988. Lithostratigraphy, biostratigraphy and sedimentary dynamics of the Lower Cretaceous deposits on the northern side of the western High Atlas (Morocco). Cretaceous Research 9, 141–158.
Roch, E., 1930. Une histoire stratigraphique du Maroc. Notes et Mémoires du Service géologique du Maroc 80, 1–440.
Roth, P.H., 1978. Cretaceous Nannoplankton Biostratigraphy and Oceanography of the Northwestern Atlantic Ocean. In: Benson, W.E., Sheridan, R.E., Pastouret, L., Enos, P., Freeman, T., Murdmaa, I.O., Worstell, P., Gradstein, F., Schmidt, R.R., Weaver, F.M., Stuermer, D.H. (Eds.), Initial Reports of the Deep Sea Drilling Project, vol. 44, pp. 731–759.
Schlager, W., 1980. Mesozoic calciturbidites in Deep Sea Drilling Project Hole 416A: Recognition of a drowned carbonate platform. In: Lancelot, Y., Winterer, E.L. (Eds.), Initial Reports of the Deep Sea Drilling Project, 50, Washington D.C. U.S. Gov. Print. Off., pp. 733–749
Schwarz, E., Buatois, L.A., 2012. Substrate-controlled ichnofacies along a marine sequence boundary: The Intra-Valanginian Discontinuity in central Neuquén Basin (Argentina). Sedimentary Geology 277–278, 72–87.
Shmeit, M., Giraud, F., Jaillard, E., Reboulet, S., Masrour, M., Spangenberg, J.E., El-Samrani, A., 2022. The Valanginian Weissert event on the south Tethyan margin: a dynamic paleoceanographic evolution based on the study of calcareous nannofossils. Marine Micropaleontology 175, 102134.
Sissingh, W., 1977. Biostratigraphy of Cretaceous Calcareous Nannoplankton. Geologie en Mijnbouw 56, 37–65.
Soua, M., 2016. Cretaceous oceanic anoxic events (OAEs) recorded in the northern margin of Africa as possible oil and gas shale potential in Tunisia: an overview. International Geology Review 58, 277–320.
Sprovieri, M., Coccioni, R., Lirer, F., Pelosi, N., Lozar, F., 2006. Orbital tuning of a lower Cretaceous composite record (Maiolica Formation, central Italy). Paleoceanography 21, PA4212.
Taj-Eddine, K., Ettachfini, El M., Rey, J., 1992. Le Berriasien et le Valanginien de l'Atlas Atlantique – Maroc. Biostratigraphie et séquences de dépôt. Géologie Méditerranéenne 19, 41–50.
Thieuloy, J.P., 1977. La zone à Callidiscus du Valanginien supérieur vocontien (Sud-Est de la France). Lithostratigraphie, ammonitofaune, limite Valanginien–Hauterivien, corrélations. Géologie Alpine 53, 83–143.
Thieuloy, J.P., Bulot, L., 1992. Ammonites du Crétacé inférieur du Sud-Est de la France: 1. Nouvelles espèces à valeur stratigraphique pour le Valanginien et l'Hauterivien. Géologie Alpine 68, 85–103.
Thieuloy, J.-P., Fuhr, M., Bulot, L., 1990. Biostratigraphie du Crétacé inférieur de l'Arc de Castellane (S.E. de la France). 1: Faunes d'ammonites du Valanginien supérieur et âge de l'horizon dit de "La Grande Lumachelle". Géologie Méditerranéenne 17, 55–99.
Vašíček, Z., 2020. *Teschenicera*s gen. nov. (Ammonoidea) and the definition of the Valanginian/Hauterivian boundary in Butkov Quarry (Central Western Carpathians, Slovakia). Acta Geologica Polonica 70, 569–584.
Wiedmann, J., Butt, A., Einsele, G., 1982. Cretaceous Stratigraphy, Environment, and Subsidence History at the Moroccan Continental Margin. In: von Rad, U., et al. (Eds.), Geology of the Northwest African Continental Margin. Springer-Verlag, pp. 366–395.
Wippich, M.G.E., 2001. Die tiefe Unter-Kreide (Berrias bis Unter-Hauterive) im südwestmarokkanischen Becken: Ammonitenfauna, Bio-und Sequenzstratigraphie. Unpublished PhD thesis, Universität Bochum, p. 142.
Wippich, M.G.E., 2003. Valanginian (Early Cretaceous) ammonite faunas from the western High Atlas, Morocco, and the recognition of western Mediterranean "standard" zones. Cretaceous Research 24, 357–374.
Witam, O., 1998. Le Barrémien-Aptien de l'Atlas Occidental (Maroc): lithostratigraphie, biostratigraphie, sédimentologie, stratigraphie séquentielle, géodynamique et paléontologie. Strata 30, 1–421.
Zühlke, R., Bouaouda, M.-S., Ouajhain, B., Bechstädt, T., Leinfelder, R., 2004. Quantitative Meso/Cenozoic development of the eastern Central Atlantic continental Shelf, western High Atlas, Morocco. Marine and Petroleum Geology 21, 225–276.

Appendix A. Supplementary data

Supplementary data to this article can be found online at https://doi.org/10.1016/j.cretres.2022.105341.